Available online at www.sciencedirect.com
ScienceDirect
Physics Reports 447 (2007) 112–143
PHYSICS REPORTS
www.elsevier.com/locate/physrep

An introductory essay on subcritical instabilities and the transition to turbulence in visco-elastic parallel shear flows

Alexander N. Morozov*, Wim van Saarloos

Instituut–Lorentz, Leiden Institute of Physics, Universiteit Leiden, Postbus 9506, 2300 RA Leiden, The Netherlands

Available online 18 April 2007
editor: I. Procaccia

Abstract

This paper is an pedagogical essay on the scenario of the instabilities and the transition to turbulence in visco-elastic polymer flows. When polymers are long, they get easily stretched by the shear present in flows, and the viscosity of the solution or melt is large. As a result, inertial effects are usually negligible as the Reynolds numbers are small but the fluid is strongly nonNewtonian due to the shear-induced elasticity and anistropy, and the slow relaxation effects. The dimensionless number governing these nonNewtonian effects is the Weissenberg number Wi. From a number of precise experiments and theoretical investigations in the last fifteen years, it has become clear that as the Weissenberg number increases, visco-elastic fluids exhibit flow instabilities driven by the anisotropy of the normal stress components and the curvature of the streamlines. The combination of these normal stress effects that drive laminar curved flow unstable and the possibilty of the elastic effects to store energy in high shear regions and to dump it elsewhere in less sheared regions, appears to be strongly self-enhancing: Instabilities and the transition to a turbulent regime driven by these elastic forces, are often found to be hysteretic and strongly subcritical (nonlinear). There are two main underlying themes of this introductory essay. First of all, that it is profitable to let one be motivated by transition scenarios in Newtonian fluids as a function of Reynolds number, when investigating possible transition scenarios in visco-elastic fluids as a function of Weissenberg number. Secondly, that the self-enhancing effects of polymer stretching will also cause subcritical instabilities in visco-elastic parallel shear flows. The aim of this paper is to introduce and discuss these issues at a pictorial level which is accessible for a nonexpert. After introducing some of the basic ingredients of polymer rheology we follow a number of the important theoretical and experimental developments of the last fifteen years and discuss the picture that emerges from it. We then turn to a discussion of recent theoretical and numerical approaches aimed at establishing whether visco-elastic parallel shear flows indeed also exhibit a subcritical transition to elastic turbulence. We show how a simple extension of the well-known condition of Pakdel and McKinley for the instability threshold of curved flows, can be extended to the nonlinear (subcritical) instability scenario of parallel visco-elastic shear flows. This extension predicts the critical amplitude for the nonlinear instability to decrease as $1/\mathrm{Wi}^2$ and to be independent of the wavenumber k of the perturbations. The fact that the threshold is k-independent over a large range of k's suggest that many modes will be excited at the same time, and hence that the instability will generally drive the flow turbulent. Implications of these results and an outlook for the future are discussed as well.

PACS: 83.60.Df; 83.60.Wc; 67.40.Vs

* Corresponding author.
E-mail address: morozov@lorentz.leidenuniv.nl (A.N. Morozov).

0370-1573/$ - see front matter © 2007 Elsevier B.V. All rights reserved.
doi:10.1016/j.physrep.2007.03.004

Contents

1. Introduction: the challenge of understanding nonlinear visco-elastic flows

It is well known that when the Reynolds number $\mathrm{Re} = VL/\nu$ increases, flows of Newtonian fluids typically follow a scenario illustrated in Fig. 1(a): (i) at small Re the flow is laminar and stable, (ii) at some intermediate value the laminar flow profile becomes unstable, so that a more complicated flow pattern develops, while (iii) at sufficiently large Reynolds numbers the flow is turbulent. Newtonian fluids are simple fluids like water and alcohol whose dynamics is described by the Navier–Stokes equations. For a fluid with kinematic viscosity ν in a geometry of linear scale L with a typical flow velocity V, the Reynolds number $\mathrm{Re} = VL/\nu$ is the ratio of the inertial term of $\mathcal{O}(V^2/L)$ and the viscous damping term of order $\nu V/L^2$ at the largest relevant scale, the scale of the flow geometry. So, since the Reynolds number measures the importance of inertial effects relative to the viscous damping effects, the typical scenario summarized in Fig. 1(a) is that as inertial terms become more and more important in normal Newtonian flows, there is a tendency to more and more complicated flow patterns and eventually turbulence. Sometimes the first transition is a transition to a nontrivial coherent flow pattern, and this transition is followed by one or more secondary bifurcations, before the turbulent regime is reached. But a direct transition from a laminar flow to a turbulent flow is also possible.

Of course, the qualitative and quantitative details of this transition scenario depend very much on the problem at hand. For example, in the Taylor–Couette geometry (a fluid confined between two concentric rotating cylinders [1–3]), the first nontrivial change when the outer cylinder is fixed while the inner one rotates with increasingly large rotation rate, is a sharp transition to Taylor vortex flow, induced by a linear instability of the laminar flow profile. When the rotation rate is increased even more, one rapidly encounters secondary bifurcations to more complicated flows and turbulence [3]. For counterrotating cylinders, there may even be a direct transition to turbulence, i.e., there is no intermediate regime with nontrivial coherent flow. This is consistent with the fact that in planar Couette flow (two parallel plates moving in opposite directions, with a fluid in between) the laminar flow is linearly stable for any Re, while a nonlinear (subcritical) transition to turbulence occurs in practice for Re of order 300–400 [4]. After all, in the limit in which

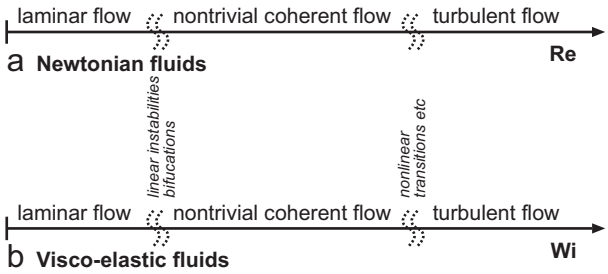

Fig. 1. Qualitiative sketch stressing the simularities between the typical scenario found in Newtonian fluids as the Reynolds number Re increases, and in visco-elastic fluids upon increase of the Weissenberg number Wi. (a) The typical scenario which is found for Newtonian fluids characterized by Re. As the Reynolds number increases, the laminar flows often first give way to nontrivial but coherent flow patterns which can be stationary (e.g., the pattern of Taylor vortices in a Taylor–Couette cell) or periodic (e.g., the Von Karmann vortex street behind a cylinder). For sufficiently large Re the flows are turbulent. Keep in mind that the intermediate regime of nontrivial coherent flows does not always exist—e.g., in pipe flow there is a direct (subcritical) transition from laminar to turbulent flow which itself is incoherent, but which nevertheless appears to be organized by coherent structures, see Section 4.1. (b) Low Reynolds number flows of visco-elastic fluids are characterized by the Weissenberg number Wi which measures the importance of relaxation, elasticity and anisotropy effects due to the visco-elasticity. The lower figure illustrates that it is profitable to think of visco-elastic fluids as following a similar scenario to more complicated flows and turbulence, upon increasing Wi, as Newtonian fluids do as upon increase of Re. Of course, in any practical situation one should keep in mind that there are important differences between the two cases and the fact that the route to turbulence followed in a particular case depends crucially on the flow geometry.

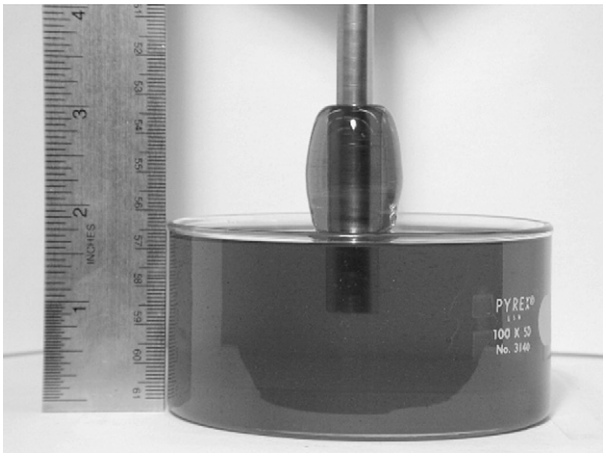

Fig. 2. Rod climbing in a solution of high molecular weight polystyrene in a Newtonian fluid: when the inner rod is rotated, the shear-induced stretching of the polymer makes them climb up the rod. Photo courtesy of G. H. McKinley (MIT), http://web.mit.edu/nnf/. A movie of this phenomenon can also be downloaded from this web page.

the gap is small and the cylinders counterrotate with the same rotation rate, Taylor–Couette flow approaches planar Couette flow. Likewise, the transition to turbulence in pipe flow is direct and nonlinear, although, as we shall discuss in Section 4.1.4, weakly turbulent flow in this geometry still appears to be organized by coherent structures [5].

In visco-elastic flows of polymeric solutions and melts, the Reynolds numbers are often quite small, since the viscosity is large. Instead, the important dimensionless number characterizing the rheology of polymers is the Weissenberg number Wi which controls the stretching of the polymers, the so-called normal stress effect, and the relaxation phenomena. When the Weissenberg number Wi becomes large, in practice larger than 1, the rheology becomes very nonNewtonian [6–11]. A simple well-known example of this is the so-called rod-climbing effect [6] illustrated in Fig. 2: in this figure the rod in the center which is immersed in the polymer solution is rotating. Due to the shear-induced stretching of the polymers, the polymer "climbs" the rod. These effects, which we will describe in more detail in Section 2.1, result in nonlinear effects on hydrodynamic length scales, as they are induced by the shear rate (the velocity gradient) in the flow being large enough, larger than the inverse of the longest polymer relaxation time. So, in visco-elastic flows the nonlinear effects do not come from inertial terms but from the elastic terms.

The question now naturally arises whether small Reynolds number visco-elastic flows will follow roughly a similar scenario as the Newtonian fluids—a laminar flow regime, followed possibly by a regime with nontrivial coherent flow patterns, then turbulence—as a function of the Weissenberg number Wi, as sketched in Fig. 1(b), and what the mechanism of destabilization would be.

Clearly, this question can only be posed and answered precisely for a given flow geometry and for a given rheological model (the so-called "constitutive equation" for the visco-elastic stresses). Nevertheless, the normal stress effect, which we think is the major mechanism of flow destabilization and transition to turbulence in visco-elastic flows, is very robust and common to virtually all polymers. Therefore, we feel that it is useful to think of this question in this broader sense, and to be guided by the analogy between well-known Newtonian scenario of Fig. 1(a) and the putative visco-elastic scenario of Fig. 1(b) when tackling a specific problem.

Simply put, the aim of this article is to introduce the reader in a pedagogical way to some of the basic open issues concerning visco-elastic flows that emerge from approaching such flows from this angle. As we shall discuss, in the last decade several key experiments have been done which demonstrate the existence of visco-elastic instabilities and turbulence and which lead us to propose that our thinking be guided by the analogy in Fig. 1. Moreover, these experiments indicate, loosely speaking, that visco-elastic flows might have an ever stronger tendency to become turbulent than normal Newtonian fluids. This forces on us the question what the typical route to turbulence of visco-elastic flows is, and whether the scenario of Fig. 1(b) is realistic. Many of the issues are still largely open, and researchers are struggling to find a way to approach them. It is therefore too early for a *review* of the subject—instead this article has more the character of an introductory *essay* aimed at bringing together evidence from various angles on how strong the tendency of visco-elastic fluids is to exhibit subcritical flow transitions. One of the main threads of this essay will be that this tendency to subcritical behavior is so strong, that also viso-elastic parallel shear flows exhibit a direct subcritical transition to visco-elastic turbulence.

Apart from the intrinsic scientific interest in exploring the similarity of the two scenarios of Fig. 1, there are also very good practical reasons to do so. If Newtonian fluid dynamics remains a challange even today, then visco-elastic flows seem to pose unsurmountable problems. First of all, at the technical level, the difficulty is that while the Navier–Stokes equations for a Newtonian fluid are simply equations for the velocity *vector* field, the rheological equations for a visco-elastic fluid involve a nonlinear "constitutive equation" for the stress *tensor*. Any calculation is therefore much harder for visco-elastic flow than for Newtonian flow, and even conceptually simple approximation schemes often lead to cumbersome expressions with many terms. Secondly, the structure of these equations is such that in flow regions with significant shear, components of the stress tensor tend to grow exponentially fast; this makes numerical simulations of such flows so hard that the difficulty of extending numerical techniques to significant Weissenberg numbers has been termed the *High Weissenberg Number Problem* [12–14]. Finally, a complicating factor is that because there are many different constitutive equations, one always faces the question to what extent a given theoretical result is an artifact of a particular constitutive equation or an explicit example of a relatively general phenomenon.

For all the above reasons, even if analogies can only help give qualitative insight into which instability scenario or route to turbulence might be possible or expected in a particular case, exploring these analogies can be of great help in studying visco-elastic flows.

Let us illustrate that following the guidance of this analogy may indeed be powerful and lead to many new questions and ideas, by telling how it led us to what will be the main underlying theme of this essay. Our interest in visco-elastic flows as a pattern formation problem arose when we posed ourselves the question "will visco-elastic flow in a parallel flow geometry (plane Couette flow, Poiseuille flow) exhibit some kind of nonlinear instability to (probably weakly) turbulent flow, just like Newtonian pipe and Couette flow become turbulent at high enough driving forces?" As we shall discuss, it has been accepted for quite some time that in flow geometries with curved streamlines (like a Taylor–Couette cell), visco-elastic flows become linearly unstable at high Weissenberg numbers, even when the Reynolds number is small [15]. These instabilities are due to the anisotropy of stress tensor, which also gives rise to the so-called rod-climbing effect of polymer solutions, shown in Fig. 2. As we will discuss in more detail in Section 4.1, if one is a bit familiar with the nonlinear (subcritical) transition to turbulence in Newtonian pipe flow or Couette flow, one naturally expects visco-elastic pipe flows to have a similar nonlinear subcritical transition to some kind of turbulent state. Simply put, one expects the laminar state to be linearly stable to perturbations of infinitesimal amplitude, but once the amplitude of the perturbation is large enough, the perturbed flow will have curved streamlines and the *curved streamlines in combination with anisotropic forces* mechanism will take over and the perturbations will grow even larger [17–20]. This is the essence of what is called a subcritical (nonlinear) transition.

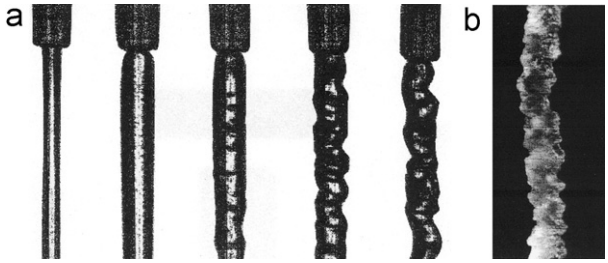

Fig. 3. Illustration of the surface irregularities that occur in the extrusion of a polymer fluid from a tube. (a) Observations made by the group of Bonn (unpublished): five snapshots of a polymer flowing out of a tube (the wider structure at the top), with the flow rate increasing from left the right. Beyond some critical flow rate (between the second and third snapshot) the "extrudate" becomes irregular. An important issue is whether these irregularities could be the result of a subcritical flow instability in the tube or whether, as is commonly believed, this behavior is always driven by instabilities at the inlet or outlet of the extruder. (b) At high flow rates the extrudate is very irregular. Larson [26] has suggested that this may be a manifestion of "turbulence without inertia". Experimental evidence for such noninertial elastic turbulence is discussed in Section 3.6. Reprinted by permission from Macmillan Publishers Ltd: Nature, copyright (2000).

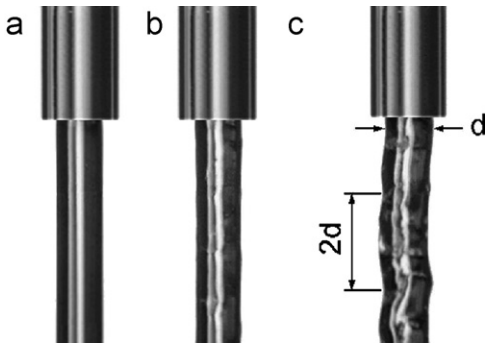

Fig. 4. Three snapshots from experiments on polymer–crosslinker system (polyvinyl alcohol/sodium tetraborate) flowing out of the tube, close to the onset of the formation of irregular behavior of the outflow. The flowrate is increasing from left to right. As indicated in the figure, the typical lengthscale of the undulations is about twice the tube diameter. From [17].

Quite surprisingly, after parallel shear flows were shown to be linearly stable in the mid-seventies of the previous century, the implicit assumption in the field seems to have been that such flows would also be nonlinearly or even absolutely stable, i.e., that even if such flows are perturbed significantly, they will return to steady laminar flow behavior. As we shall discuss later in Section 4, the final verdict on this issue is not yet in, but there are both strong theoretical and numerical indications that indeed there is indeed a nonlinear flow instability, with a threshold which decays rapidly (as $1/\mathrm{Wi}^2$) with Weissenberg number. Moreover, we shall show that a simple back-of-the-envelope extension of the linear stability criterion of curved flows predicts that the threshold is wavenumber-independent, suggesting that the instability normally will give rise immediately to turbulence.

The question concerning the nonlinear stability of parallel shear flows actually has immediate practical and technological relevance. To see this, take a look at some of the photos in Figs. 3 and 4 of a polymer melt flowing out of a tube shown at the top of the figure. In the five snapshots in Fig. 3(a), the flow rate increases from left to right; the picture clearly illustrates that beyond some rather well-defined flow rate (close to the one near the middle snapshot), the outflow (the "extrudate" in industrial terms) shows undulations whose amplitude increases rapidly with increasing flow rate. As Fig. 3(b) illustrates, at high enough flow rates the flow appears to be chaotic or turbulent [26]. In fact, various recent high-precision experiments on visco-elastic model fluids have given overwhelming evidence for the presence of turbulence in visco-elastic fluids at low Reynolds numbers [21–25]. To contrast this with the inertia-driven turbulence in Newtonian flows, Larson has coined the term "*turbulence without intertia*" or *elastic turbulence* [26].

Although we will focus here on the basic issue of polymer flow stability and the onset of turbulence, we note that the effects illustrated in Fig. 3 are directly relevant technologically: the standard way of making polymer fibers and sheets in industry is extrusion, in which the molten polymer is forced through a small opening and subsequently cooled to obtain

the final product. Since undulations of the extrudate like those shown in the Figs. 3 and 4 are unwanted, the occurrence of such instabilities is *the* rate-limiting factor for such extrusion processes [7,27–30]. A detailed understanding of these types of phenomena has remained elusive for already over 40 years: the earliest documented attempts date back at least to the 1960s [21], when the use of polymer fibers became widespread. Although it is clear that in some cases instabilities at the outlet of the extruder are at the origin of melt fracture phenomena, if indeed polymer pipe flow itself exhibits a nonlinear instability, these will in some sense pose a fundamental barrier to avoiding melt fracture instabilities. In fact, as we shall discuss later, if the instability is subcritical (nonlinear), it is likely that in practice extrusion instabilities are strongly coupled to the nonlinear instabilities in the pipe, as the latter need to be triggered by an perturbation of sufficiently large amplitude.

As we will focus in this paper on elasticity-dominated phenomena at low Reynolds numbers, we will not touch here on the well-known problem of drag reduction, the reduction of drag of Newtonian turbulence by adding small amounts of polymers to the fluid [31–33]. Neither will we review theories for well-developed elastic turbulence, as we focus here on the nonlinear instability that will drive a laminar parallel shear flow unstable.

The outline of the paper is as follows. In Section 2 we first introduce at an elementary level some of the basic ingredients of polymer rheology. We discuss the shear-induced stretching of the polymers, the effects it gives rise to, as well as the dimensionless numbers associated with it. We then introduce some of the constitutive equations for polymer rheology. In Section 3 we will then follow a number of important theoretical and experimental developments of the last fifteen years. The picture that emerges in particular from these experiments is that the tendency of normal stress effects to drive laminar curved flow unstable together with the possibilty of the elastic effects to store energy in high shear regions and to dump it elsewhere in less sheared regions, is strongly self-enhancing. It results in a strong tendency for such flows to exhibit subcritical instabilities and to rapidly give rise to elastic turbulence. In Section 4 we then turn to a discussion of recent theoretical and numerical approaches aimed at establishing whether visco-elastic parallel shear flows also exhibit a subcritical transition to elastic turbulence. We close the paper with a brief discussion of the implications of these results and of the outlook for the future.

2. Some basic elements of visco-elastic flows

In this section we introduce some of the basis ingredients of polymer rheology.

2.1. A polymer melt or solution under shear becomes an anisotropic elastic fluid with relaxation

What makes a polymer melt or solution so different from a regular Newtonian fluid? Simply put, the answer is that a polymer fluid is a *visco-elastic fluid*: as illustrated in Fig. 5, once shear gradients $\dot{\gamma} \equiv \partial v_x(y)/\partial y$ become large enough, the elastic polymers become stretched and acquire an average orientation. As a result, shear makes the fluid *anisotropic*. For most polymer solutions and melts, the most important effect [6] is the build-up of a difference $N_1 \equiv \tau_{\mathrm{p},xx} - \tau_{\mathrm{p},yy}$

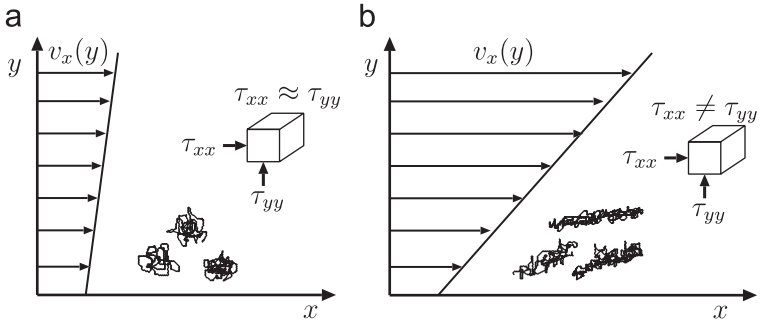

Fig. 5. Qualitative sketch of the stretching and orientation of polymers in a simple shear flow $v_x(y)$ in the x direction. (a) For small gradients $\dot{\gamma} \equiv \partial v_x(y)/\partial y$, the polymers are hardly deformed—they are circularly symmetric on average. (b) At large shear rates $\partial v(y)/\partial y$ the polymers become stretched and oriented on average. As a result, the normal stresses become different: $\tau_{\mathrm{p},xx} \neq \tau_{\mathrm{p},yy}$.

in the normal stress[1] $\tau_{p,xx}$ along the flow direction x and the normal stress $\tau_{p,yy}$ in the direction along the shear direction y (see figure). For simple shear flows of Newtonian fluids, $\tau_{xx} = \tau_{yy} = 0$ and thus $N_1 = 0$, but for polymers N_1 increases quadratically in the shear rate $\dot{\gamma}$. For viscous polymers, inertial effects are small since the Reynolds number Re is inversely proportional to the viscosity. Since the viscosity of polymers increases rapidly with the polymer length [34,35], the Reynolds number quickly goes down with the degree of polymerization. On the other hand, the stretching effects illustrated in Fig. 5 quickly go *up* with the degree of polymerization. Hence the relevant dimensionless number characterizing the rheology of sufficiently long polymers is therefore not the Reynolds number Re, but the so-called *Weissenberg number* Wi, the ratio of the normal stress difference N_1 and the shear stress $\tau_{p,xy}$ due to the polymers:

$$\mathrm{Wi} = \frac{|N_1|}{|\tau_{p,xy}|} = \frac{|\tau_{p,xx} - \tau_{p,yy}|}{|\tau_{p,xy}|}. \tag{1}$$

For $\mathrm{Wi} \ll 1$ the fluid behaves essentially like a regular Newtonian fluid, but for Wi of $\mathcal{O}(1)$ or larger the visco-elastic properties make polymer solutions and melts into complex fluids with a rheology very different from ordinary fluids: The peculiar phenomena of visco-elastic liquids we are interested in all happen for $\mathrm{Wi} > 1$ when the normal force differences are larger than the shear forces.

The stretching of the polymers which brings about the anisotropy means that the fluid gets elastically loaded: When the polymers stretch, elastic energy is stored in the sheared fluid. This elastic energy can be released after the fluid element has been adverted to other regions where the shear-induced stretching forces are smaller. Thus, an important mechanism of elastic energy transfer is introduced.

A third important aspect associated with the stretching is that the polymer liquid has an internal relaxation time: If shear changes, it takes the polymers some time to adapt to the new shear stresses. Thus the fluid effectively has some memory.

The anisotropy, elasticity and memory effects are in essence three different manifestations of one and the same effect—they are all intimately connected and can not be tuned very easily independently: the longer the polymer, the larger the relaxation time, the sooner the shear-induced anisotropy occurs, and the weaker the strength of the elastic spring which gets loaded.

As for Newtonian fluids, the shear stress (τ_{xy} in the above example) is linear in the shear rate $\dot{\gamma}$ for small $\dot{\gamma}$. The normal stress difference, however, increases quadratically in $\dot{\gamma}$—this reflects the fact that when the shear gradient in Fig. 5 has changed sign, the effect on the normal forces due to the polymer stretching remains the same. Since the Weissenberg number is according to (1) the ratio of the normal stress difference over the shear stress, Wi increases linearly in $\dot{\gamma}$ for small $\dot{\gamma}$:

$$\mathrm{Wi} \sim \dot{\gamma} \quad (\text{small } \dot{\gamma}). \tag{2}$$

Let λ be the characteristic (longest) relaxation time of the polymers. We can think of the constant λ as the relaxation time of stretching of the polymers, the time scale on which a stretched polymer blob will relax to its equilibrium scape in the absence of shear. Since the shear rate $\dot{\gamma}$ has the dimension of inverse time, we can thus introduce a second dimensionless number, the Deborah number [6] defined as

$$\mathrm{De} = \lambda\dot{\gamma}. \tag{3}$$

Of course, real polymers are characterized by many relaxation times [34,35]—we should think of λ as being the longest relaxation time which governs the long scale relaxation of the polymer blob. Moreover, as we already indicated above, anistropy, elasticity and relaxation are intimately related effects, and in the simplest approximation there is only one constant λ governing these effects. Likewise, as we shall see below, in the simplest constitutive equations for the polymer stress tensor τ_p, frame invariance dictates that the strength of all the nonlinear and relaxation terms is governed by only one parameter λ with the dimension of time. Moreover, in these constitutive equations, the Weissenberg number Wi is strictly proportional to $\dot{\gamma}$ for all shear rates, and in these cases the Deborah number De and Weissenberg number Wi are essentially the same, up to a numerical factor of order unity. In a way, it is somewhat surprising how well a single time

[1] We use, following the book by Bird et al. [6], the notation to denote the polymer stress tensor by τ_p; in the physics literature, σ is more common for a stress tensor.

scale model often works, to capture the gross rheological features. This is a signal that often the normal stress effects and the elasticity are the dominant effects governing the flow. Nevertheless, one should keep in mind that in general the two dimensionless numbers are not the same and that many polymer-pecific effects (e.g. shear thinning, which is not modeled by the simplest constitutive equations) can play a role.

For polymer solutions which are sufficiently dilute that the viscosity of the solvent can not be neglected, there is an additional dimensionless number β associated with the ratio of the solvent viscosity η_s to the polymer viscosity η_p,

$$\beta = \frac{\eta_s}{\eta_s + \eta_p}. \tag{4}$$

When very small amounts of polymers are added to a solvent, e.g. to achieve drag reduction [31–33], β is very close to 1. We are here especially interested in the opposite regime $\beta \ll 1$ where the overall viscosity is dominated by the polymers and the Reynolds number is small.

2.2. Constitutive equations

The simplest model to capture the three basic ingredients of polymer rheology discussed above and which hence has become the working horse of theoretical studies of visco-elastic polymer flow [6,9,10]) is the so-called Oldroyd-B model; it is defined by the following "constitutive equation" for the polymer shear stress tensor τ_p in terms of the shear rate tensor $\nabla\mathbf{v}$ through

$$\tau_p + \lambda[\partial\tau_p/\partial t + \mathbf{v}\cdot\nabla\tau_p - (\nabla\mathbf{v})^\dagger\cdot\tau_p - \tau_p\cdot(\nabla\mathbf{v})] = -\eta_p(\nabla\mathbf{v} + (\nabla\mathbf{v})^\dagger). \tag{5}$$

This constitutive equation is characterized by one single relaxation time λ. Indeed, the first two terms in (5), $\tau_p + \lambda\partial\tau_p/\partial t$, make any changes in τ_p relax on the timescale λ. The second and the third terms, $\partial\tau_p/\partial t + \mathbf{v}\cdot\nabla\tau_p$, describe advection of the stress along the flow streamlines. The other two nonlinear terms (with $(\nabla\mathbf{v})^\dagger$ indicating the transpose of the tensor $\nabla\mathbf{v}$) are in fact required to form a frame-independence time derivative of the polymer stress tensor.[2] We refer to a detailed discussion of the necessity to incorporate these terms to the literature [6,10].

The above equation for τ_p in terms of the shear rate have to be supplemented by the Navier–Stokes equation

$$\rho[\partial\mathbf{v}/\partial t + \mathbf{v}\cdot\nabla\mathbf{v}] = -\nabla p - \nabla\cdot[\tau_s + \tau_p], \tag{6}$$

where τ_s is the stress tensor of the solvent which is given by the usual Newtonian expression

$$\tau_s = -\eta_s(\nabla\mathbf{v} + (\nabla\mathbf{v})^\dagger). \tag{7}$$

It is customary to take the fluid (with density ρ) to be incompressible so that

$$\nabla\cdot\mathbf{v} = 0. \tag{8}$$

The above equations are referred to as the Oldroyd-B model [6,10].

If there are no polymers so that τ_p=0, then Eq. (6) simply reduces with (7) and (8) to the incompressible Navier–Stokes equation for the solvent. In this equation, the "only" nonlinearity is the nonlinear term $\mathbf{v}\cdot\nabla\mathbf{v}$ on the left-hand side of Eq. (6), as the "constitutive equation" for the solvent is the linear relation (7) between τ_s and the shear $\nabla\mathbf{v}$. The importance of this nonlinear term is measured by the Reynolds number Re. In the opposite limit, when the solvent is unimportant ($\beta \to 0$ in (4), a limit which is referred to as the *Upper Convected Maxwell* (UCM) model),[3] the structure is very different. This is most easily seen in the zero Reynolds number limit, when (6) reduces simply to the *linear* equation

$$\mathrm{Re} \to 0: \quad 0 = -\nabla p - \nabla\cdot\tau_p. \tag{9}$$

[2] All the terms between square brackets together form the so-called upper convected derivative [6].

[3] This is because when all the nonlinear terms are ignored, (5) is simply the linear Maxwell model for visco-elastic response. The term between square brackets is simply the so-called *upper convected derivative* that arises in a frame-invariant formulation.

so that all the nonlinearities now come from the constitutive equation (5). In fact, the nonlinearities are in this case bilinear in $\nabla \mathbf{v}$ and τ_p. In other words, when we go from a Newtonian fluid to a highly viscous polymer fluid, the nonlinearities shift from the Navier–Stokes equation to the constitutive equation. In between, the equations are of mixed character.

We noted above that it is immediately obvious that relaxation behavior is incorporated by the time derivative term in the constitutive equation (5). That the other two basic ingredients of polymer rheology, anistropy and elasticity, are also properly described by the Oldroyd-B or UCM model, is less obvious at first sight, but can be checked by analyzing simple flows like the laminar profiles in plane Couette or pipe Poiseuille flow. It is then found [6] that these models do indeed give rise to normal stress terms and a first normal stress difference N_1 proportional to $\dot{\gamma}^2$ *through the nonlinear terms in the constitutive equation* (5). Coming from the continuum level description, the intimate connection between relaxation, elasticity and anisotropy is dictated by the requirements of frame-invariance: this requirement dictates that all the nonlinear terms in (5) come with the specific prefactors ± 1, and hence that in the simplest approximation, these effects are all governed by the single relaxation parameter λ in the model. Starting from a more microscopic level, this constitutive equation can be derived for noninteracting dumbbells connected with Hookean springs [6,10].

On the one hand, because of the tensor nature of the field τ_p, even this model, which is essentially the simplest one for polymer rheology, is very difficult to analyze in practice—almost any analysis of a nontrivial flow problem has to rely on a substantial amount of numerical work. On the other hand, the Oldroyd-B and UCM model still do exhibit some shortcomings, which require one to go to more complicated extensions in a number of circumstances. The most important of these shortcomings is that in elongational flows like $(v_x, v_y, v_z) = \dot{\epsilon}(2x, -y, -z)$, the model breaks down at $\lambda\dot{\epsilon} > 1/2$. This breakdown is essentially due to the fact that this constitutive equation is based on modeling a polymer as a dumbbell with an infinitely extensible elastic spring: for $\lambda\dot{\epsilon} > 1/2$ the elongational flow is strong enough to drive the two sides of the dumbbell infinitely far apart from one another. This nonphysical behavior can be avoided by extending the model so as to make the springs nonlinearly elastic with a finite maximum extension—the so-called FENE-P model—or by including a nonlinear saturation term in (5); an example of this is the so-called Giesekus model [6].

We note in passing that these rheological models are notoriously hard to simulate at moderate and large Wi [12]—the High Weissenberg Number Problem already referred to above. The basic reason for this can easily be seen as follows, and is again related to the sensitivity of elongational flow regions: in regions of elongational flow the nonlinear $\tau_p \cdot \nabla \mathbf{v}$ term and its adjoint lead to exponential growth in component of τ_p in the terms between brackets of (5), which makes a regular numerical code prone to instabilities. One way around this, proposed recently [13,14], is to simulate what amounts to the logarithm of the polymer stress tensor, whose growth is only linear in time in these regions.

2.3. Model polymer fluids and optimal models for the various regimes

As we saw above, in the simplest approximation one arrives at constitutive equations with essentially only one parameter, the relaxation time λ, which we think of as the relaxation time of a polymer in response to shear. It is remarkable that it is possible in practice to make model polymers, so-called Boger fluids, whose rheology conforms well to the Oldroyd-B model [36]. Moreover, even though there are certainly a number of polymer-specific effects involved, even the rheology of technologically relevant polymers is often captured *grosso modo* by simple constitutive equations.

If one, however, wants to reproduce rheological properties of a particular polymer better than just qualitatively, one has to take into account the nature of the fluid. UCM, Oldroyd-B and FENE-P are common examples of models derived from considering a single dumbbell in a flow and, therefore, work only for very dilute solutions. Semidilute solutions and melts are better described by Giesekus, PTT, Larson-Marrucci models, etc. [6,11]. Often one has to include a spectrum of relaxation times to enhance agreement with the experimentally observed rheological properties. Moreover, one has to keep in mind that not every model performs equally well in a given type of flow. One example is the Oldroyd-B fluid which qualitatively describes rheological properties of a dilute polymer solution in shear flow, but fails to predict physical values of the viscosity in extensional flow—it diverges when the relaxation time of the polymer times the extension rate exceeds 0.5.

In what follows, we focus on the Oldroyd-B model since it contains the most important rheological ingredient for viscoelastic instabilities and turbulence—the normal-stress effect.

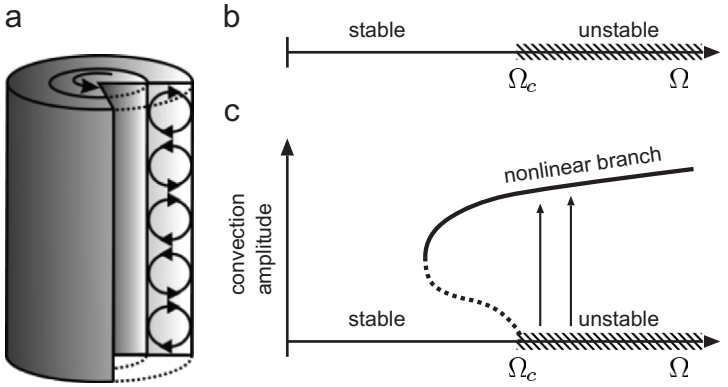

Fig. 6. (a) Sketch of a Taylor–Couette cell. (b) Sketch of a rotation rate axis, with a critical number a la Larson marked on it. (c) Qualitative sketch of the subcritical scenario as found by Groisman and Steinberg [42].

3. Polymer flow instabilities and "turbulence without inertia"

3.1. How it all began: visco-elastic instabilities in a Taylor–Couette cell

Although systematic studies of visco-elastic flows date back many years,[4] in many ways it is fair to mark the beginning of the more modern perspective with the 1990 paper by Larson et al. [38]. These authors analyzed the stability of zero-Reynolds number flow in a Taylor–Couette cell using the Oldroyd-B model discussed above. A Taylor–Couette cell is sketched in Fig. 6(a); it consists of a fluid between two co-axial cylinders which can rotate independently.

As we noted already in the introduction, the Taylor–Couette cell is one of the most basic experimental setups to study inertia-driven instabilities and turbulence in Newtonian fluids [1–3]. The phase diagram as a function of the rotation rates of the inner and outer cylinder is very complicated, exhibiting many patterned and turbulent states [3]. One nice aspect of the Taylor–Couette cell is that when the gap d between the cylinders is small, one approaches plane Couette flow when the cylinders are rotating with equal but opposite speed.

Larson et al. [38] noted that this system is also an ideal system to study visco-elastic instabilities in the limit that the Re is small. Technically, the advantage is that the system is translation invariant along the cylinder axis (assuming the cell to be very long) so that one can consider Fourier modes for the spatial modulation along the axis.[5] Since in the $\mathrm{Re} \to 0$ limit inertial effects are unimportant, only the difference in rotation rates of the two cylinders matters, so one can for instance take the outer cylinder fixed and study the stability of the laminar azimuthal flow as a function of the rotation rate Ω of the inner cylinder.

For the Oldroyd-B model, Larson et al. [38] predicted there to be a clear *linear instability* of the visco-elastic laminar azimuthal base flow: As sketched in Fig. 6(b), there is a critical rotation rate Ω_c,

$$\Omega_c^2 = \Lambda \frac{k_z d}{\lambda} \frac{d}{R_\mathrm{i}}, \tag{10}$$

where R_i is the radius of the inner cylinder, d is the gap between two cylinders, k_z is the wavelength of the velocity modulation along the cylinders, and Λ is a dimensional constant which is related to the temporal eigenvalue and which depends on De, k_z and β. Beyond Ω_c, the laminar flow profile is *linearly unstable* to periodic modulations along the axis of the cylinder with the wavelength k_z, indicating that beyond the threshold the flow would exhibit a banded structure very reminiscent of the Taylor vortices which form first in the Newtonian case when passing a critical rotation rate. Clearly, the critical value (10) depends on the gap-to-radius ratio of the cell d/R_i: when the radius goes to infinity, the instability disappears as the threshold Ω_c shifts to infinity. This is consistent with old results [39] that show that visco-elastic planar Couette flow is linearly stable fow all Wi. The important interpretation which then emerged from

[4] See, e.g., [21] and references in [6]. A very readable historical perspective can be found in [37].

[5] In addition, one can make a number of simplifying approximations if the gap between the cylinders is much less than the radii of the cylinders.

this work and later extensions [9,40,41] was that when the inertial effects are unimportant, visco-elastic flows can exhibit an elasticity-driven instability when the flow-lines are curved. We will summarize the physical argument in the following subsection.

Using Boger fluids, the first experiments in [38] already confirmed the existence of such an elastic instability. In more detailed experiments a few years later, Groisman and Steinberg [42] found that the predictions for the threshold rotation rate Ω_c also agreed quantitatively quite well with their experimental findings. However, they also found that the instability is *subcritical*, as sketched in Fig. 6(c): once the flow pattern sets in, finite-amplitude nontrivial flow patterns continue to exist when the rotation rate Ω is reduced *below* the critical value Ω_c. In the experiments, the resulting so-called "di-whirl" convection patterns are quite localized and they continue to exist down to $\Omega \simeq \Omega_c/2$. Thus, these experiments show two important results: (i) They confirm that with appropriately prepared model polymer solutions, one can make quantitative contact between experiments and theoretical predictions for Oldroyd-B fluids. (ii) They are the first solid experimental evidence that instabilities in visco-elastic fluids tend to be *subcritical*, i.e., nonlinearly enhanced.

3.2. Curvature of the base flow and anisotropic elasticity: the general mechanism of linear instabilities

It has become clear from the work described above that in the small Reynolds number limit, visco-elastic flows generally tend to become *linearly unstable* due to normal stress effects when the streamlines are curved [9,15,38]. To understand why such flows are unstable, first consider a flow with curved streamlines, as illustrated in Fig. 7(a). When the Weissenberg number is larger than about 1, the polymer is stretched by the shear gradients. The inner part of the (artist impression of) the polymer on the left stretches and rotates, because of the larger curvature of the stream lines and the larger shear near the center, towards the situation of the second polymer charicature on the right. Clearly this polymer is therefore being pulled towards the center—this is the origin of the rod-climbing effect of Fig. 2. To understand the mechanism of a finite-wavelength instability in confined curved flow, consider next Fig. 7(b). Again, for Weissenberg numbers larger than about 1, there is a significant normal stress effect which tends to pull fluid element in towards regions of higher curvature of the flow lines. Now, consider a small perturbation of the flow, so that the perturbed streamlines become as indicated with the solid lines in Fig. 7(b) (the unperturbed ones are indicated with dashed lines). Some of the fluid elements move outwards a bit, some move inwards towards regions of larger shear. The effective force pulling the latter fluid elements inwards thus increases, whereas the effective force on the fluid elements moving outwards decreases, as the size of the arrows indicating the effective force indicates. Clearly, the effect may thus be self-enhancing, implying that the flow is unstable if the forces are large enough. Moreover, we expect the instability to set in earlier the larger the Weissenberg number, and the larger the curvature of the streamlines is.

In Fig. 7(b), we consider a wavy perturbation *along* the streamlines. In the laminar flow state of the Taylor–Couette geometry, there are curved streamlines "stacked on top of each other" all along the axial direction. The same type of reasoning as above leads to the conclusion that a perturbation with a wavevector along the axis, so that the flow moves inwards somewhat at some levels and moves outwards in regions in between, should become unstable too. Which instability is strongest is a quantitative question which can only be settled with a full-fledged linear stability

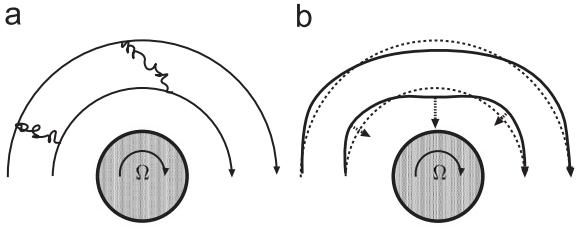

Fig. 7. Qualitative sketch of a flow situation with curved streamlines. At large enough Weissenberg numbers when there are significant normal stress differences, the normal forces tend to pull a fluid element in towards the region of largest curvature of the streamlines and largest flow rate. (a) Illustration of the origin of the rod-climbing effect: under the flow a polymer like the one on the left, is stretched and oriented by the flow to a situation like the one on the right. Effectively, the polymer is pulled inwards. (b) The full lines indicate small perturbations of the streamlines around the unperturbed, shown by dashed lines. Fluid elements which are displaced inwards towards regions of larger curvature are pulled in even more, fluid elements which are displaced outwards are being pulled in less. Hence the flow is unstable.

analysis. As Larson et al. [38] found, the perturbation with wavevector along the axis usually goes unstable first, and as a result the first nontrivial state is a banded flow structure, reminiscent of Taylor vortices. There are, however, regions of parameter space where perturbations with different symmetry are more unstable.

Pakdel and McKinley [15,16] have shown that many of the instability criterions based on the balance between curvature and normal stress effects can be summarized by an expression of the form

$$\frac{\ell}{\mathscr{R}}\frac{|N_1|}{|\tau_{\mathrm{p,shear}}|} > M^2. \tag{11}$$

Here ℓ is the length scale over which a perturbation moving along a streamline will decay; in other words, $\ell = U_{\mathrm{sl}}\lambda$, where U_{sl} is the typical velocity along the streamlines and λ, as before, is the polymer relaxation time. Furthermore, $\mathscr{R}$ is the typical radius of curvature of the base flow, while in the ratio of the normal stress term N_1 and the shear stress $\tau_{\mathrm{p,shear}}$ we recognize the Weissenberg number Wi introduced in (1). Finally, M is a constant, which depends on the flow geometry, and which typically ranges from 1 to 6 [15,16].

Note that (11) is actually the most natural dimensionless criterion that incorporates all the necessary ingredients of instabilities driven by the combination of anisotropic elastic normal forces and curvature. The term $N_1/\tau_{\mathrm{p,shear}} = \mathrm{Wi}$ is the dimensionless measure of the anisotropy of the normal forces—the larger Wi the larger this driving term. In addition, the smaller the radius of curvature $\mathscr{R}$, the stronger the instability, hence the term $1/\mathscr{R}$. Finally, the decay length ℓ should not only be there for dimensional reasons, but is also taking into account the physical effect that the longer a perturbation survives, the longer it can help to drive the flow unstable. Thus, on hindsight, one could almost have guessed the general form of this condition. We will refer to (11) as the Pakdel–McKinley condition, and will later in Section 3.5.3 extend its interpretation so as to have it predict the threshold for subcritical instabilities in parallel shear flows as well.

Finally, it should be stressed that the instability condition (11) has not really been derived; instead, the status of the condition is more that Pakdel and McKinley [15,16] observed that all know instability criteria could be recast in this form, which is physically most reasonable.[6] We are tempted to think that this condition should be viewed as a reasonable expression valid at large enough Weissenberg numbers and not too small radii of curvature. Thus, as it stands, the above expression suggests that even at small Wi an instability could set in if the streamlines are sufficiently curved. We consider it more likely, however, that such instabilities are suppressed at small Wi, and that the above expression should be thought of as a good asymptotic large-Wi rule of thumb which is accurate for sufficiently large Wi, larger than at least 1. Clearly, this issue needs to be addressed in more detail in the future.

3.3. Ring-like and spiral waves in a plate–plate geometry

Let us now turn to a discussion of important experiments on spiral patterns in a plate–plate experiments. In such experiments, the typical example of which is sketched in Fig. 10(a) below, one has two cylindrical plates of which the upper one can rotate. The gap between the cylinders, which is of constant thickness, is filled with the elastic fluid. The flow patterns can be visualized from the top or bottom plate.

Byars et al. [44] have performed an extensive series of experiments on the flow patterns that form in such experiments on two realisations of the Boger fluid: two different concentrations of polyisobutylene dissolved in polybutene and tetradecane. Fig. 8 shows an example of a typical observation: the first nontrivial flow patterns that form are either concentric ring patterns or spiral patterns roughly halfway between the center and the outer edge. These patterns are comprised of vortices that rotate in the gap between two plates bringing the fluid from one plate to the other and back, and are wound up in such a way that they look like either rings or spirals from above. The emergence of these concentric vortex-like flow patterns is in full agreement with the linear stability analysis by Öztekin and Brown [46]. These authors studied the stability of the laminar base flow for the Oldroyd-B model and found that both rings and spirals bifurcate from the laminar state, though spirals are slightly more unstable. Recently, Schiamberg et al. [47] have systematically studied various patterns occurring in the plate–plate flow geometry and transitions between them.

[6] Moreover, in complicated flow geometries, instabilities typically set in regions where the effective value of the ratio on the left of (16) is largest [43].

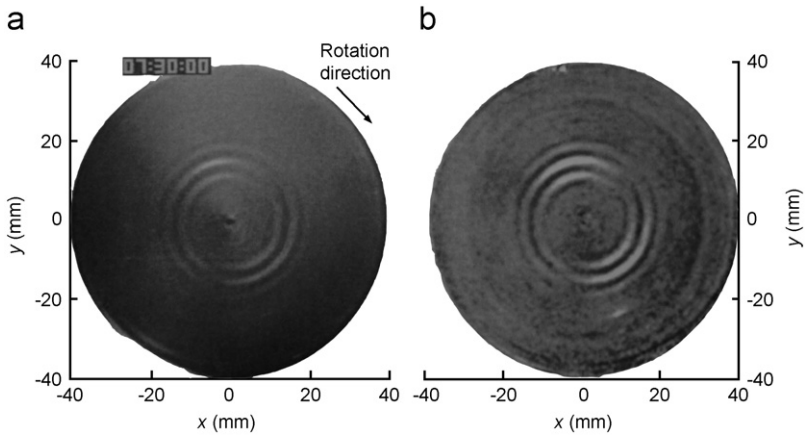

Fig. 8. Example of a spiral flow pattern observed by Byars et al. [44] in a plate–plate geometry. The photo on the left shows the raw experimental observation viewed from the top. In the picture on the right the pattern is enhanced using digital subtraction.

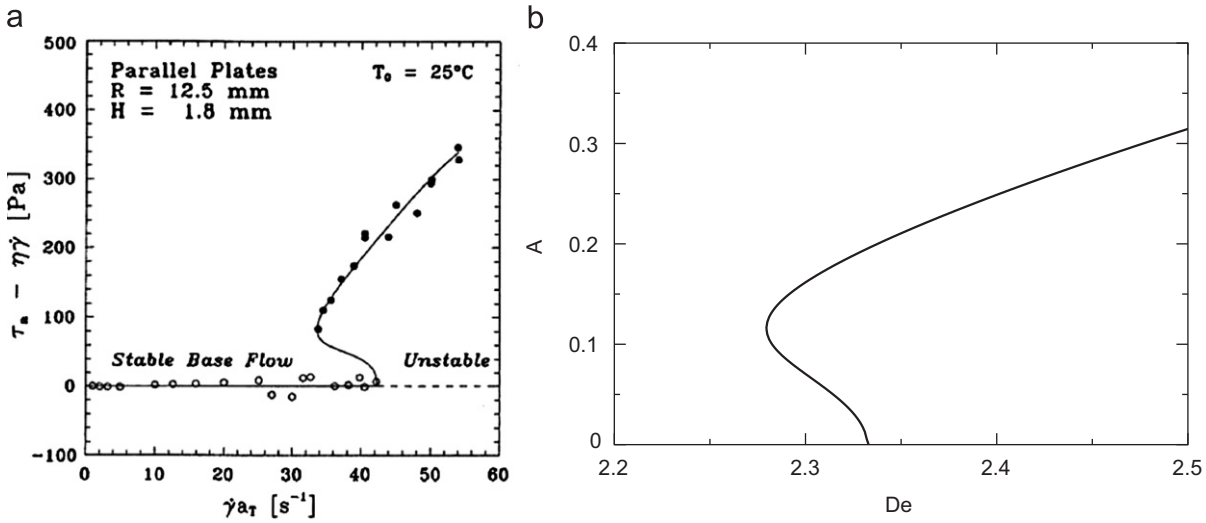

Fig. 9. (a) Experimental data from Byars et al. [44] showing that the transition to ring-like convection patterns in visco-elastic fluids is often subcritical. Along the vertical axis the excess shear stress on the upper plate is plotted as a function of the rotation rate of the upper plate. The excess shear stress is the total shear stress on the upper plate minus the one in the laminar state, calculated from the fluid viscosity and the rotation rate of the plate. The open symbols denote data points in the laminar base state, the filled symbols the state where convection rings form. The data give clear evidence for the transition to be subcritical, with the saddle-node point where the convection branch starts located about 20% below the instability threshold of the laminar base state. (b) A weakly nonlinear amplitude expansion for this experimental situation predicts subcritical behavior which is similar to the experimental findings [45]. *A* is the amplitude controlling the strength of the secondary flow, and *De* is the Deborah number. Note that the linear stability analysis predicts instability to set in at *smaller* shear rates than experimentally observed [46].

An experimental finding which is worth stressing from our perspective is that also these experiments showed a tendency for hysteresis, and hence for subcritical behavior. An example of some of these experimental results is plotted in Fig. 9(a). In this plot, the enhancement of excess torque necessary to rotate the upper plate at a give rate, is plotted as a function of the rotation rate. As the data show, one can follow the existence of this nontrivial flow branch to values of the rotation rate some 20% below the critical value where the instability sets in, and the amplitude of the excess torque is finite at the critical value of the linear instability. Both of these are clear signatures that the bifurcation to the nontrivial flow patterns is subcritical.

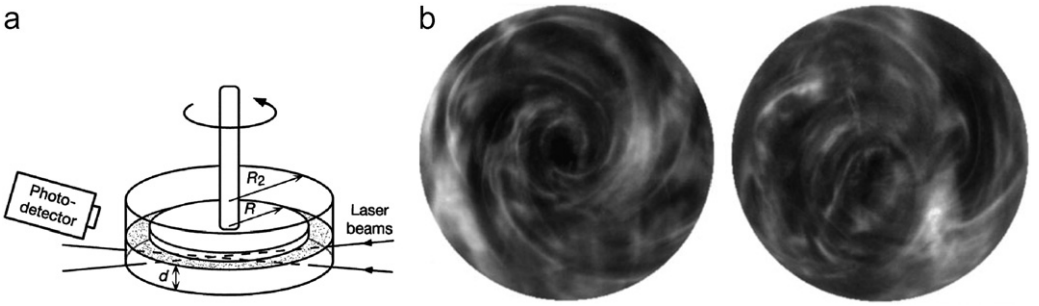

Fig. 10. (a) Sketch of the plate–plate geometry used by Groisman and Steinberg in their experiments [22]. (b) Two snapshots of turbulent flow in the experiment at Wi = 13 and Re = 0.7 [22]. Reprinted by permission from Macmillan Publishers Ltd: Nature, copyright (2000).

As we mentioned above, amplitude expansions [49–51] are a well-established technique to study the pattern dynamics just above the threshold of a supercritical transition. Also when the transition is weakly subcritical ("weakly" meaning that the jump at the transition is not too large, in some appropriate way of measuring this),[7] one can study the near-threshold behavior of the patterns. Motivated by the experimental results shown in Fig. 9(a), we have therefore studied the near-threshold convection using an amplitude equation to fifth order. As the data Fig. 9(b) show, such an expansion gives results consistent with the experimental findings: the transition is subcritical, and, depending on the parameter range, the saddle-node point ("nose") of the nonlinear branch is in the range 1–20% below the critical value of the linear instability.

3.4. Elastic turbulence in a plate–plate geometry

The next important step in our story is the finding of Groisman and Steinberg [22,23] who revisited the plate–plate geometry some six years ago. Their setup is sketched in Fig. 10(a). They used a dilute solution of high molecular weight polyacrylamide in a viscous sugar syrup with a relaxation time $\lambda = 3.5$ s. Conceptually, these experiments are very much like the ones on the ring and spiral patterns discussed above, but when Groisman and Steinberg pushed the experiments to slightly large Wi at low Reynolds numbers (Re is typically smaller than 1 in their experiments) they found a strong tendency to turbulent behavior. Two typical snapshots of the swirly flow in these experiments are shown in Fig. 10(b).

The data is analyzed quantitatively in Figs. 11 and 12. In Fig. 11 the shear stress on the top plate, normalized by the value of the shear stress the fluid would have if the flow would have been laminar at the same rotation rate, is plotted as a function of the rotation rate. The range of shear rates presented in Fig. 11 corresponds to Weissenberg numbers in the range 1–25, the range where elastic and normal stress effects are important.

The data sets labeled 1 and 2 correspond to the viscoelastic fluid at different sizes of the gap between the plates: $d = 10$ and 20 mm, respectively (see Fig. 10(a)). The third data set represents the pure solvent. For the data sets 1 and 2, the curve of the total normalized stress first rises slowly above 1. This corresponds to the regime discussed above where there are regular concentric ring type convection patterns and spirals. Upon increasing the rotation rate (and hence Wi) the curves then quickly rise sharply. This is the regime where the visco-elastic turbulence, which is visualized in Fig. 10, sets in. Thus, there is a very rapid transition to turbulence in these experiments, and as the arrows indicate, this transition to turbulence is hysteretic, and hence subcritical, too: when the rotation rate is decreased slowly once the flow is turbulent, the turbulent state disappears at a slower rotation rate than the one where the rapid transition to turbulence occurred upon increasing the rotation rate. Obviously, the data set 3 does not exhibit any rise of the shear stress above the laminar value indicating that the phenomenon observed is purely due to the presence of the polymer.

[7] Mathematically, an amplitude equation $A_t = \epsilon A + \delta|A|^2 A - |A|^4 A$ applies in the subcritical regime $\epsilon < 0$, $|\epsilon| \ll 1$ provided $\delta = \mathcal{O}(\sqrt{\epsilon})$ so that all terms on the right are of the same order, with $|A| \sim |\epsilon|^{1/4}$.

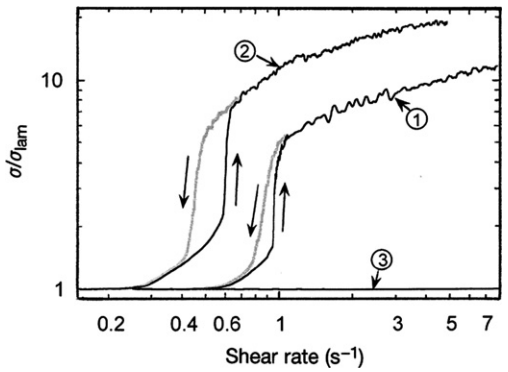

Fig. 11. Shear stress on the top plate in the plate–plate experiments by Groisman and Steinberg [22] as a function of rotation rate of the upper plate. The shear stress is normalized by dividing by the shear stress if the flow would be laminar, calculated using the viscosity of the solution. Three different data sets are shown: the curves labeled 1 and 2 are for the flows with the distance between the plates $d = 10$ and 20 mm, respectively. Curve 3 corresponds to the pure solvent without polymers. Reprinted by permission from Macmillan Publishers Ltd: Nature, copyright (2000).

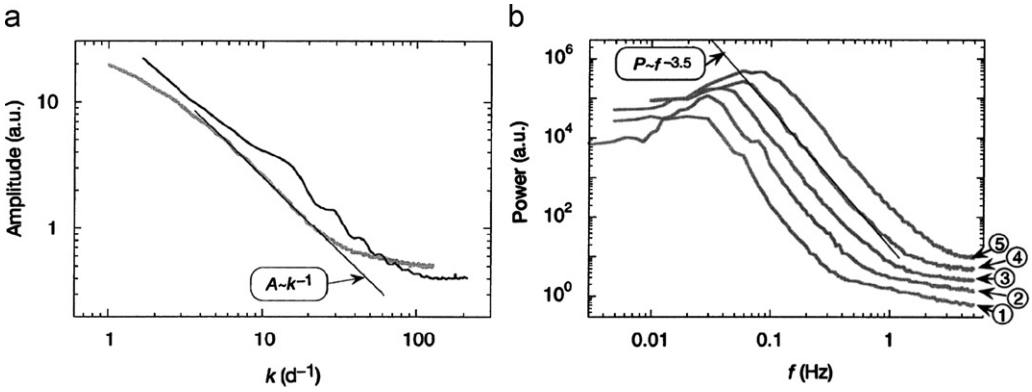

Fig. 12. Spatial and temporal spectra as measured in the plate–plate experiments by Groisman and Steinberg [22]. Reprinted by permission from Macmillan Publishers Ltd: Nature, copyright (2000). (a) Average Fourier spectra of the brightness profiles along the diameter (thin black line) and along the circumference at a radius $2d$ (thick gray line). Note that since the brightness in Fig. 11 does not provide any information about local velocity, the value of the scaling exponent has no physical meaning. (b) Power spectra of velocity fluctuations taken at different shear rates $\dot{\gamma} = 1.25$, 1.85, 2.7, 4.0, and 5.9 s^{-1} above the transition.

The strong tendency for visco-elastic flow to exhibit self-enhanced turbulent behavior is illustrated by the large enhancement of the measured shear stress over the laminar value: Note that the data are plotted on a logarithmic scale along the vertical axis, and that the enhancement of the shear stress is easily a factor 10. As Groisman and Steinberg [22] point out, in Newtonian turbulence one has to go up to Reynolds numbers of order 10^4 to get such very large enhancements!

That the states which to the eye appear to be turbulent in Fig. 10(b) indeed have all the features of turbulence is demonstrated by the spatial and temporal spectra shown in Fig. 12: the spectra show clear power law scaling over at least a decade. Recent theories for this power law scaling [48] are in good agreement with the exponents found in these experiments.

Taken together these experiments by Groisman and Steinberg have been instrumental in identifying *turbulence without inertia* or *elastic turbulence*, words coined by Larson [26], as an important and well-defined problem associated with visco-elastic fluids. All indications of these experiments are that polymer fluids tend to become turbulent very easily even at low Reynolds numbers. This means that once there is a bit of nontrivial flow, the normal forces and curvature of the streamlines tend to *enhance* the flow—this gives raise to subcritical behavior.

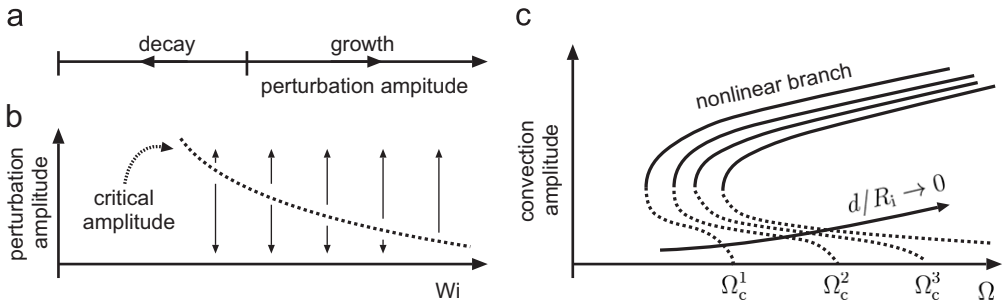

Fig. 13. (a) Qualitative sketch of the stability situation in the case of a subcritical instability. Under the dynamics, small amplitude perturbations decay to the zero-amplitude fixed point, but beyond a critical amplitude, perturbations grow. (b) If there is a subcritical bifurcation for visco-elastic flow, the critical amplitude is expected to come down with increasing Wi. (c) For visco-elastic Taylor–Couette flow, the threshold rotation rate Ω_c shifts to larger values when the gap ratio d/R_i is decreased. This naturally leads us to suspect that bifurcation-from-infinity scenario of (b) for visco-elastic plane Couette flow.

3.5. Parallel shear flows and anisotropic elasticity: subcritical instabilities

3.5.1. The argument for linear instabilities in curved flows predicts subcritical instabilities in parallel flows

As we saw above, when the base flow has curved streamlines, then the anisotropic visco-elastic forces will make the base flow *linearly unstable* for large enough Weissenberg numbers. When a state is linearly unstable, this means that some perturbation modes of arbitrarily small amplitude, whose dynamics is governed by linearizing the rheological equations about the base state solution, will grow exponentially in time. However, it is immediately clear that the well-known and generally accepted argument for the instability mechanism of visco-elastic flows also implies that parallel shear flows—flows in geometries whose streamlines are straight, like plane Couette flow, or plane and pipe Poiseuille flow—should be *nonlinearly unstable*: Since the streamlines of the unperturbed problem are straight, a perturbation of infinitesimal amplitude is not sufficient to drive the flow unstable. However, with a perturbation of *finite* amplitude the streamlines of the perturbed flow are curved, and once the amplitude is large enough, the perturbed flow should be unstable for large enough Weissenberg number, as sketched in Fig. 13(a). We might say that we need a perturbation on top of a perturbation to drive the flow unstable, and hence the flow is nonlinearly unstable. Moreover, if there is such a nonlinear instability, the nonlinear driving force for the instability will increase with increasing driving force, so the critical amplitude of the perturbation that separates decaying perturbations from growing ones, will *decrease* as a function of Wi. Hence we typically expect a situation as sketched in Fig. 13(b): it is as if there the critical threshold "bifurcates from infinity".

As we shall discuss in Section 4.1, in plane Couette flow or Poiseuille pipe flow of Newtonian fluids, the laminar base flow is also linearly stable for all Reynolds numbers, but there is a transition to turbulence at large Reynolds numbers Re. Very much as in Fig. 13(b), the threshold for the transition to turbulence decreases with increasing Re (experimentally as Re^{-1} [53]). This situation is sometimes also termed a "bifurcation from infinity", a term already alluded to above. Note, however, that this name sometimes obscures the fact that the best way of understanding the real physics is not by thinking about it as a bifurcation from infinity! The transition to turbulence in Newtonian pipe flows is a good illustration of this, as we shall discuss in Section 4.1.

3.5.2. Digression on the differences between supercritical and subcritical bifurcations

Let us digress briefly on the word subcritical instability, and the difference with the more common case of a supercritical bifurcation. When the base state of a system exhibits a linear instability, at the point where the instability sets in a branch of nonlinear solutions bifurcates off. This situation is sketched in Fig. 14(a). This nontrivial branch of nonlinear solutions, which in the case of a finite wavelength instability of the base state describes a branch of patterned solutions, exits in the *supercritical* regime, the regime where the base state is unstable. This case is therefore referred to as a supercritical bifurcation. Since as sketched in Fig. 14(a) the amplitude of these patterns (i.e., the strength of the modulation of the dynamical fields) grows continuously beyond the bifurcation point, just beyond threshold these solutions can be analyzed perturbatively. These methods are called amplitude expansions [49–51], and they can be used to analyze both the existence and the dynamics and competition of solutions in the weakly nonlinear regime. They thus

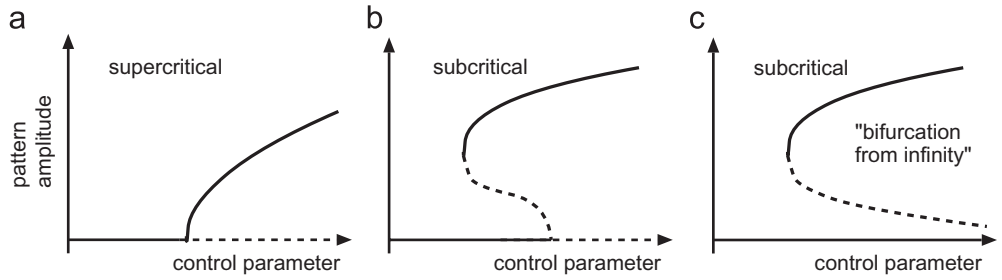

Fig. 14. General illustration of the bifurcation diagrams at (a) a supercritical instability, (b) a subcritical instability and (c) a subcritical instability that "bifurcates from infinity". In these plots, dashed curves indicate branches of solutions which according to bifurcation theory are unstable. Note, however, that "stability" means here stability with respect to growth or decay of the amplitude. In a realistic pattern forming system, the nonlinear branches of solutions can be unstable to other finite wavelength perturbations. This happens in fact for the nonlinear solutions that govern weak turbulence in Newtonian—see Section 4.1.

provide an essentially complete description of the nontrivial near-threshold dynamics. Usually, among the nontrivial pattern solutions that bifurcate off from the base state there are classes of stable nonlinear solutions, but this is not always the case.[8]

Usually, the word "subcritical instability" refers to situations like those of Fig. 14(b), where the branch of patterns which bifurcates off from the point where the base state becomes unstable exists below this critical value (hence "subcritical"). The solutions on this branch are unstable and hence dynamically irrelevant—the branch of stable and hence physically nonlinear pattern solutions is the one corresponding to the upper branch, which bifurcates off from the so-called "saddle-node" point, the "nose" on the left where the unstable and stable branch merge. The above continuation argument shows that this case and the "bifurcation from infinity" case of Fig. 14(c), where the base state never becomes unstable, are often intimately related. The important common feature of both cases is that in the subcritical range where the base state is linearly stable, a *finite* perturbation of the flow state is needed to drive the base flow unstable. We will therefore refer generally to both of these cases as a subcritical bifurcation. Moreover, one should keep in mind that in complicated situations, the nonlinear state associated with the upper branch may not always be a nonlinear attractor. But even then these weakly unstable nonlinear solutions can organize much of the chaotic or weakly turbulent nonlinear dynamics (see footnote 8).

So it is important to keep in mind that subcritical bifurcation diagrams like those in Fig. 13(a,b) are actually very qualitative, contrary to those associated with so-called supercritical bifurcations, where the physically relevant branch originates from the linear instability. When a system exhibits a true linear instability, there is a single well-defined eigenmode of the linear stability operator, which goes unstable first. At a supercritical bifurcation, the nonlinearities are saturating, and as a result just above the threshold the amplitude of the modulation of the new patterns is small (see Fig. 14(a) below); accordingly, one can describe the dynamics of the system just above the threshold in terms of amplitude modulations of this most unstable mode [49–51]. When there is a linear instability in a case where the nonlinearities enhance (rather than saturate) the growth, the pattern amplitude is already finite when the base state becomes linearly unstable. When the subcritical nature is strong, the linear instability (if it exists) is not very relevant for the existence of dynamics of the patterns that typically already arise before the instability of the base state occurs. Typically, the location of the saddle-node point where the nonlinear branch arises (bifurcates) is more important. In other words, a subcritical instability is, by its very nature, governed by all kinds of nonlinear self-enhancing interactions and so there is almost never a simple approximation scheme that allows one to explore the infinite dimensional phase space of interactions in all details, and determine which direction corresponds to the smallest threshold. Thus, in practice, one can explore such situations, in theoretical studies as well as in experiments, only for a given class of perturbations. Theoretically, the simplest possibility is usually to consider spatially periodic perturbations of fixed wavelength of the base flow, and explore the nonlinear stability of

[8] For example, if one considers a supercritical bifurcation to traveling wave states, the dynamics just above threshold is governed by the so-called Complex Ginzburg Landau equation. There are parameter regimes of this equation where the traveling periodic patterns that this equation describes, are all linearly unstable [49–51]. The weakly chaotic dynamics that then emerges is then still governed by the Complex Ginzburg Landau equation, however. In the chaotic regime of this equation, weakly unstable nonlinear solutions (so-called homoclon solutions) are the building blocks of the chaotic dynamics [52]. The fact that weakly chaotic nonlinear dynamics is organized by weakly unstable exact solutions appears to have its counterpart in the weakly turbulent regime of Newtonian fluid dynamics, discussed in Section 4.1.

the base flow as a function of the amplitude of these periodic perturbation. This is what is done in the theoretical analysis described later in Section 4.2. Experimentally, one usually applies a well-characterized localized perturbation and varies its amplitude (see, e.g., [53]). The advantage of numerical studies is that in principle both types of perturbations can be applied.

As we shall discuss in Section 4.1 below, Newtonian turbulence provides very nice illustrations of the above discussion: while in plane Poiseuille flow the base state becomes linearly unstable at $\mathsf{Re} = 5772$, so that the situation is like sketched in Fig. 14(b), the transition to turbulence usually sets in at $\mathsf{Re} = \mathcal{O}(1000)$. Actually, the nonlinear branch that bifurcates from the point where the linear instability occurs, is different from the one that governs the transition to turbulence! In practice, therefore, there is not a big difference between this case and the transition to turbulence in plane Couette and pipe Poiseuille flow, where there is no linear instability of the base flow, so that the scenario of Fig. 14(c) applies. Moreover, in all these cases, there is no branch of stable nonlinear solutions, although the weakly turbulent regime near threshold does appear to be organized by exact nonlinear traveling wave solutions which are weakly unstable. We will come back to this in Section 4.1.

3.5.3. A simple estimate of the critical amplitude based on the Pakdel–McKinley condition

Let us return to the subcritical visco-elastic instabilities. It is easy to obtain a simple estimate for the critical amplitude of the periodic perturbations that will drive a parallel shear flow nonlinearly unstable by extending the interpretation of the Pakdel–McKinley condition (11) following the lines laid out also in [54]. The Pakdel–McKinley condition is normally viewed as the instability criterion for when base flows with a fixed finite radius of curvature $\mathscr{R}$ go *linearly instable* upon increasing Wi. However, as we have seen, the physics of the nonlinear finite-amplitude instability is just the same as that of the linear instability of curved base flows, and hence the threshold condition should be governed by exactly the same dimensionless group. We can implement this idea for fixed Wi by considering a base flow with straight streamlines in the x-direction, so that the curvature of the streamlines of the base flow is zero, and perturb the flow with a periodic transverse modulation with wavenumber k. This situation is sketched in Fig. 15 for the case of Couette flow, both in the lab frame in which the plates are moving, and in the frame moving (almost) with the speed of the upper plate.

It will turn out to be most convenient to formulate the threshold condition in terms of the dimensionless amplitude of a modulation with wavenumber k of the shear rate at the wall,

$$A_{\mathrm{shear}}(k) = \frac{\partial v_x/\partial y|_{\mathrm{wall}}}{\dot{\gamma}}, \tag{12}$$

where $\dot{\gamma}$ is the shear rate at the wall of the unperturbed shear flow. The easiest way to arrive at the threshold condition is to view the perturbation in the frame moving with the upper plate velocity as sketched in Fig. 15(b). In this frame,

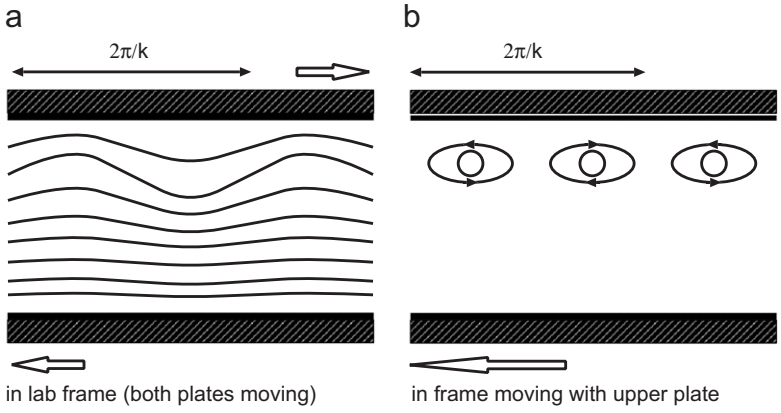

Fig. 15. Initial periodic perturbations of parallel shear flows near the wall, used in the argument to estimate the critical amplitude for the nonlinear instability. The case shown here is for plane Couette flow. The perturbation is viewed in the lab frame in (a) and in (b) in the frame moving (almost) with the speed of the upper plate. The oscillatory motion of the streamlines in the fixed frame simply looks like a periodic vortex-like motion in the moving frame. The insight that these vortices are localised near the plates is based on the fact that the eigenmodes of the stability operator are strongly peaked in a region of extent $1/k$ near the walls.

the perturbed flow consists of a vortex-type pattern with wavelength $2\pi/k$, so the radius of curvature $\mathscr{R}$ of the *perturbed* streamlines is of order π/k:

$$\mathscr{R} \approx \frac{\pi}{k}. \tag{13}$$

Moreover, in line with the fact that the eigenmodes of the linear stability operator of the base flow are strongly peaked over a distance of order $1/k$ near the wall, the typical velocity $U_{\rm sl}$ in this vortex-type motion is approximately

$$U_{\rm sl} \approx \frac{1}{k}\left.\frac{\partial v_x}{\partial y}\right|_{\rm wall} = \frac{\dot\gamma}{k} A_{\rm shear}(k). \tag{14}$$

Thus we have for the relaxation length ℓ in the Pakdel–McKinley condition (11)

$$\ell \approx \frac{1}{k}\mathsf{Wi} A_{\rm shear}(k), \tag{15}$$

where we made the approximation $\mathsf{Wi} \approx \mathsf{De} = \dot\gamma\lambda$ which in practice is a good approximation, as we discussed after the definition of the Deborah number (3). Upon substitution of these estimates into the Pakdel–McKinley condition (11), we obtain for the critical amplitude of periodic modulations of the shear flow, beyond which the flow is expected to be unstable

$$A^{\rm c}_{\rm shear} \approx \frac{M^2}{\mathsf{Wi}^2} \quad \text{independent of } k, \tag{16}$$

where as before M is some number which, based on the observations of Pakdel and McKinley [15,16], one naively expects to be in the range 1–6. While this condition can be derived most easily in the frame moving with the plates, analysis in the lab frame leads to the same conclusion, as it should of course.[9]

To our knowledge, this estimate, put forward also in [54], has not appeared before, and we are not aware of any previous tests of this result either. We will discuss semi-analytical tests as well as numerical tests of this condition in Sections 4.2 and 4.3. A very important aspect of this condition is that the threshold is predicted to be independent of k. We shall see that this k-independence over a significant range of k-values is confirmed by the semi-analytical amplitude expansion to be discussed in Section 4, but it is already important to stress here that the above argument is only correct for wavelength shorter than the plate spacing d in plane Couette or plane Poiseuile, or the pipe diameter in pipe Poiseuille flow, hence for $k \simeq 2\pi/d$. Moreover, there will of course also be a large-k cutoff as well, the cutoff associated with the scale of the polymers at which the continuum model will break down. In practice, this scale is several orders of magnitude smaller, so we expect a large range of k-values over which the threshold is roughly k-independent. This of course strongly suggest that once the instability sets in, the flow will tend to become turbulent, since many modes are expected to be excited at the same time [54].

Two final remarks. First of all, as we discussed at the end of Section 3.2, the Pakdel–McKinley condition is probably only realistic for sufficiently large Wi, large enough that there are significant normal stress effects. For this reason, we do not consider it realistic that it seems to suggest a nonzero threshold amplitude for any nonzero Wi. Secondly, we note that we already warned before to be aware of what type or perturbation is applied in a given situation. Likewise, it is important to keep in mind that the extension of the Pakdel–McKinley condition indicates that the natural threshold condition is not in terms of the stress perturbation but in terms of the *critical amplitude* $A^{\rm c}_{\rm shear}$ *of the modulation of the shear rate at the wall*, as this translates most directly in the amplitude of the modulation of the streamlines. In translating this condition of the shear perturbation at the wall into a modulation of the streamlines, we simply used the additional insight that the eigenmodes of the linear stability operator are strongly peaked near the walls over a distance $1/k$.

---

[9] In the lab frame, the horizontal velocity v_x near the wall is of order of the velocity $U_{\rm plate}$ of the upper plate and the modulation of the velocity v_y will to a good approximation be sinusoidal, $v_y \approx A_{v_y}\sin kx$, where $A_{v_y} \approx A_{\rm shear}\dot\gamma/k$. As a function of time, this implies $v_y \approx A_{v_y}\sin(kU_{\rm plate}t)$, so the vertical spatial modulation Δy of the streamlines is $\Delta y \approx A_{v_y}\cos(kx)/(kU_{\rm plate})$. The curvature of the streamline is simply equal to the second derivative of this expression with respect to x, hence $1/\mathscr{R} \approx A_{v_y}k/U_{\rm plate}$. Using that ℓ in this case simply equals $U_{\rm plate}\lambda$ since the velocity along the streamlines is dominated by $U_{\rm plate}$, we get $\ell/\mathscr{R} \approx A_{v_y}k \approx A_{\rm shear}\dot\gamma\lambda$ leading finally again to the same functional form (16), albeit with a slightly different value of M due the missing factor of π in this naive estimate.

Table 1
Critical values Wi_c for the onset of melt fracture phenomena according to Pahl et al. [27]. For comparison, viscosity of water is about 10^{-3} Pa s

Material	η, Pa s	Wi_c
Silicon Oil BW 400	1.21×10^2	4.74
Silicon Oil AK 2×10^6	2.02×10^1	4.36
Silicon Oil AK 5×10^5	6.23×10^0	4.79
Silicon Oil M 2×10^5	5.25×10^0	4.57
LDPE 1800 S	6.94×10^1	4.41
PMMA	3.50×10^2	4.62
PE	1.46×10^2	4.97
SB	3.27×10^2	4.53
ABS 90	1.92×10^2	4.74
PS 143 E	3.00×10^1	4.38
HDPE 5261 Z	2.07×10^3	4.68
PIB 10	4.10×10^0	5.24
PA N 12	1.75×10^1	4.37
Epoxy resin	5.91×10^1	4.39

3.5.4. Subcritical instability in plane Couette flow as a continuation of the Taylor–Couette flow in the small gap limit

Another way to arrive at the conclusion that visco-elastic plane Couette flow has a subcritical instability is as follows. As we already remarked before, if we take a Taylor–Couette cell whose cylinders are counterrotating with the same rotation rate, we can continuously approach plane Couette flow by taking the gap-to-radius ratio d/R_i to zero. For any value of this ratio, the flow is linearly unstable for $\Omega > \Omega_c$ given by (10). At the same time the experimental finding that the transition is subcritical suggests that for any nonzero value of d/R_i the bifurcation diagram looks as sketched in Fig. 13(c). Since the threshold Ω_c shifts to the right to infinity when we approach the case of plane Couette flow by reducing the gap ratio $d/R_\mathrm{i} \to 0$, it is then natural to expect the bifurcation diagram of Fig. 13(b) for plane Couette flow. In other words, the results on visco-elastic instabilities in Taylor–Couette geometries *naturally lead us to suspect the bifurcation from infinity scenario* to apply to planar Couette flow. And if Poiseuille flow and plane Couette flow are as similar for visco-elastic flows as they are for Newtonian flows,[10] the same scenario is expected to apply to visco-elastic Poiseuille flow as well.

3.6. The onset of melt–fracture type phenomena: a bulk rheological instability?

In the introduction, we already drew attention to the melt–fracture type phenomena [27–30] shown in Figs. 3 and 4: When the flow out of an extruder becomes too fast, the extrudate invariably develops unwanted undulations. As can be clearly seen from Fig. 3(a) the strength of these undulations continues to grow with increasing flow rate, and at very large flow rates the extrudate looks completely irregular as if it is frozen-in turbulence (Fig. 3(b)). There is a whole zoo of phenomena which can be observed [55], and some of these effects (like the short-wavelength irregularities commonly referred to as "sharkskin instability") are believed to be caused by stick–slip like instabilities at the outlet of the extruder. Nevertheless, there are strong indications that a more generic mechanism does underly many of these observations. Indeed, Pahl et al. [27] have documented the onset of this behavior in terms of the critical Weissenberg number Wi_c for the flow in the extruder for a large number of technologically relevant polymers. Their results are summarized in Table 1 below.

From these data, Pahl et al. have concluded that melt fracture type phenomena set in at a critical Weissenberg number $\mathrm{Wi}_c = 4.63 \pm 0.26$ [27]. One should take the error bars quoted for these results with a grain of salt—in most cases, the normal stresses are not measured directly but inferred from the first normal stress coefficient extrapolated from other data—and the rheology of many polymers from this diverse range can undoubtedly not be captured simply by a UCM or Oldroyd-B model (e.g., because they show shear thinning and a small second normal stress difference). The fact

[10] One can continuously interpolate between these two via Dean–Taylor flow—see [41].

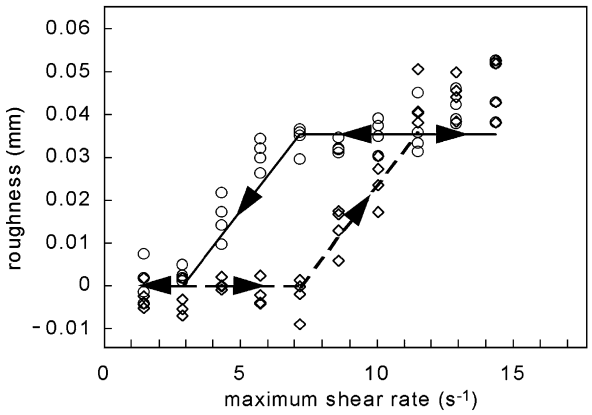

Fig. 16. Root mean shear of the fluctuations of the outflow in the experiments shown in Fig. 4 as a function of the maximum shear rate of the flow in the tube. From [17].

that they nevertheless all exhibit a very robust transition to irregular flow behavior at a rather well-defined Weissenberg number is indicative that this transition is either due to or strongly coupled with a bulk rheological transition.

It appears that since Poiseuille flow was shown to be *linearly stable* by Ho and Denn in 1978 [40], the possibility of a bulk rheological transition in the extruder as the driving mechanism of melt fracture type phenomena has been largely ignored in the field. The dominant interpretations that have emerged are in terms of stick–slip phenomena at the wall [28], instabilities at the outlet of the extuder [28,30] or polymer-specific effects [55]. Although there is no doubt that in some cases one of these phenomena is the root cause of the instability, none of these observations can explain the main observation by Pahl et al. [27] that essentially all data point at a rather well-defined critical value $\mathrm{Wi} \approx 4.8$ of the Weissenberg number, which is a *bulk rheological parameter* (Fig. 16).

As we have already argued above, we expect parallel visco-elastic shear flows like Poiseuille flow to exhibit a subcritical instability to some modulated or weakly turbulent flow state. This scenario will be developed further in Section 4. If this scenario is corroborated by future investigations, it will clearly have important implications for our understanding of melt fracture type phenomena: It would mean that a basic nonlinear flow instability would stand in the way of suppressing these irregularities in the outflow. Even then, however, one should keep in mind that because of its subcritical nature, this instability will in practice be strongly coupled with instabilities at the inlet or outlet that have been observed: such instabilities could trigger the perturbations necessary to drive the flow in the extruder unstable. In other words, if visco-elastic bulk pipe flow would be absolutely stable, inlet instabilities would damp out in sufficiently long pipes, whereas if there is a true subcritical flow instability, an inlet flow instability would trigger irregular flow in the pipe and hence make itself felt throughout the extruder. In this sense, the various effects may be strongly coupled, which makes it difficult to make a precise prediction. In other words, if there are, e.g., inlet perturbations of a given amplitude or intrinsic apparatus noise, then the resulting critical Weissenberg number is the one at which the critical amplitude branch crosses this prescribed value. This is illustrated in Fig. 17.

Whatever the origin of melt fracture is, Bonn et al. [17] have presented evidence that the transition *is* indeed subcritical, because they observed hysteresis. They measured the root mean square of the fluctuations in the cross-section of the outflow in the experiment of Fig. 4. In Fig. 16 this "roughness" of the cross-section is plotted as a function of the maximum shear rate at the wall in these experiments. In the regular laminar flow regime, this roughness is immeasurably small, so it is a simple way to characterize the irregularities of the outflow quantitatively. As indicated by the arrows in the figure, when the flow rate is slowly increased (diamond symbols), the melt fracture irregularities develop only at much higher flow rates than if one slowly decreases the flow rate (circles), starting from the phase where the irregularities are present.

3.7. The emerging picture

The picture that clearly emerges from the various experiments that we have discussed is that when the Weissenberg number Wi in curved visco-elastic flows becomes somewhat larger than one, laminar flows are very prone to transitions

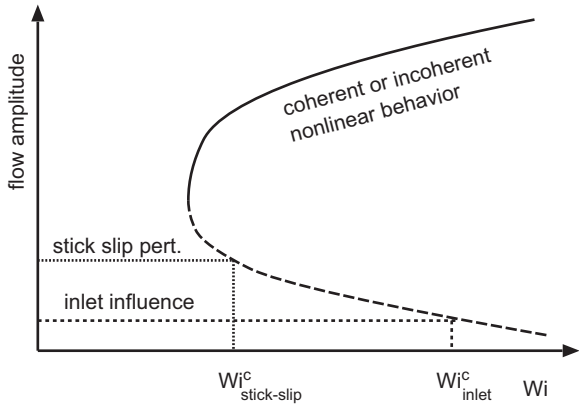

Fig. 17. Qualitative sketch of how the presence of a particular noise or perturbation level would give rise to a transition at a finite Weissenberg number Wi^c. The dashed lines indicate two hypothetical examples of levels of a perturbation amplitude, one due to stick-slip, the other from inlet perturbations. The first one leads to a critical Weissenberg number $Wi^c_{stick–slip}$, the second one to Wi^c_{inlet}.

to regular patterns or even turbulent flows. In most cases, the transition is subcritical: already at the instability threshold finite-amplitude flow patterns emerge, and there is a clear tendency to hysteretic effects. This implies that the nonlinear flow states can be followed into a subcritical range of the control parameter (usually a rotation rate). Moreover, coherent patterned states appear to be rather the exception than the rule—if they exist, they only do so in a small parameter range. They quickly give way to elastic turbulence, noninertial turbulence driven by elastic effects. Moreover, once a nontrivial flow exists, it is difficult to get rid of: both the instabilities and the turbulence tend to self-enhance—apparently, the possibility of an elastic fluid to store elastic energy in highly sheared regions and to release this energy again in less sheared regions has a strong tendency to give a positive feedback on the flow.

This strong tendency of elastic effects to give positive feedback makes it likely that parallel shear flows, like pipe Poiseuille flow, also show a strong tendency to exhibit nonlinearly unstabilities to modulated states which are probably weakly turbulent. This idea is simply a natural extension of the accepted argument that it is the combination of curved streamlines and elastic effects that drives the linear instabilities in curved flow geometries. The extension of the Pakdel–McKinley linear instability criterion to the nonlinear instabilities driven by finite amplitude modulations of parallel shear flows fully confirms this simple intuitive idea as well. Moreover, it predicts that the threshold rapidly decreases, as $1/Wi^2$, with increasing Weissenberg number, and that the instability threshold is independent of the wavenumber k over a large range of wavenumbers. This latter finding is again strongly suggestive of a rapid transition to fully developed turbulence, once a flow is perturbed beyond the instability threshold.

Unfortunately, there are to our knowledge at present no controlled experiments to test this subcritical transition scenario convincingly in detail. In the next section we will discuss the recent theoretical and numerical evidence for this scenario, as well as its experimental and theoretical implications.

4. Do visco-elastic flows in parallel shear geometries indeed exhibit a subcritical instability?

We presented in the previous section several arguments and circumstantial evidence that laminar visco-elastic flows in parallel shear geometries, which are known to be linearly stable [39,40], will exhibit a nonlinear subcritical instability of the type sketched in Fig. 13(b). In this section we will discuss some recent theoretical and numerical work aimed at determining whether this scenario is indeed correct.

In the introduction and Fig. 1 we argued that it is useful to let one be guided in the research on visco-elastic fluids by the scenarios and analogies in the fluid dynamics of regular Newtonian fluids. In this particular case, fluid dynamics provides both a historical lesson and, possibly, a guiding principle. The unitiated reader may wonder why the issue of the nonlinear stability of parallel shear flows has been dormant so long and why it is apparently so difficult to settle it convincingly. For these readers, the historical lesson from fluid dynamics is that even there some of the most important experimental and theoretical progress on the transition to turbulence in pipe flows was made in the last decades [5,53], more than hundred years after the original experiments of Reynolds that already identified a coexistence and

nonlinear competition between laminar flow and turbulence. Moreover, we do think that the recent developments in fluid mechanics may well turn out to become the guiding principle for approaching the visco-elastic flow problem. We will therefore start by briefly reviewing these developments before turning to visco-elastic flows.

4.1. The transition to turbulence in Newtonian flows: a guiding analogy

4.1.1. Is the presence or absence of a linear instability relevant?

One of the first lessons from studies of plane Couette and Poiseuille flow and Poiseuille flow in pipes is that it is in fact quite irrelevant that plane Poiseuille flow becomes linearly unstable at $\mathrm{Re} = 5772$ while plane Couette flow and pipe Poiseuille flow are linearly stable for all Re, since under usual circumstances plane and pipe Poiseuille flow exhibit a transition to turbulence at $\mathrm{Re} \simeq 1000$ and 2000, respectively; plane Couette flow usually becomes turbulent around $\mathrm{Re} = 350$. Thus, formally the bifurcation diagram of plane Poiseuille flow corresponds to the situation of Fig. 14(b) while plane Couette and pipe Poiseuille flow correspond to the "bifurcation from infinity" diagram of Fig. 14(c). But in practical situations when the transition occurs at much lower Reynolds numbers this difference is hardly of relevance.

Of course, the difference is relevant for the following: in accord with the fact that laminar pipe Poiseuille flow is linearly stable for all Re, it turns out to be possible, by carefully machining the experimental setup so as to minimize all perturbations, to avoid turbulence in pipes to Reynolds numbers of order 10^5. In plane Poiseuille flow, it will never be possible to succeed the stability limit $\mathrm{Re} = 5772$, of course. But the transition to turbulence at $\mathrm{Re} = \mathcal{O}(1000)$ is not affected by the presence or absence of an instability at much larger Re.

4.1.2. Scaling of the instability threshold for large Re

The discussion of the large-Re scaling of the amplitude necessary to drive the laminar flow unstable in the case of pipe Poiseuille flow and plane Couette flow, has been a long-standing issue. There is general agreement on a power-law scaling $\sim \mathrm{Re}^{-\gamma}$ with $\gamma \geqslant 1$ [4], but different approaches give different values of the exponent (see, for example, [56,57]). Recent experiments [53] clearly exhibit a scaling with $\gamma = 1$ over at least a decade in Reynolds numbers. This Re^{-1} scaling indicates that the threshold is basically determined by the balance of the linear viscous decay terms and the nonlinearities in the Navier–Stokes equations that drive the flow unstable.

The scaling of the stability boundary of the laminar base flow state has recently been studied in detail by Eckhardt et al. [58], who not only recovered the overall Re^{-1} scaling of this boundary, but also found clear indications that on a fine scale there is substructure. The existence of such a fine scale structure is in agreement with the interpretation of weak turbulence in terms of a self-sustaining cycle between weakly unstable coherent structures, which we review below in Section 4.1.4.

In comparison with the Newtonian case, the nature of the nonlinear terms in the visco-elastic constitutive equations is very different: the inertial nonlinearity in the Navier–Stokes equation is quadratic, while the nonlinearity in the UCM and Oldroyd-B models is bilinear in the velocity and stress. Also the physical mechanisms underlying the nonlinear instabilities of parallel shear flows is very different. Hence it need not surprise us that the extension of the Pakdel–McKinley condition, discussed in Section 3.5.3, predicts a decrease of the threshold as $1/\mathrm{Wi}^2$, while the threshold for the transition to turbulence in the Newtonian case falls of as $1/\mathrm{Re}$.

4.1.3. Nonnormality of the linear stability operator and the transient amplification of initial perturbations

Both in the Newtonian case and in the visco-elastic case, the linear stability operator of these parallel base flows is strongly nonHermitian. It has become realized [59] in the past decades that since the eigenvectors in such cases are non-normal, a typical initial disturbance will first get transiently amplified according to the linearized equations, before it will eventually, at long times, decay. In the Newtonian problem the amplification is typically a factor Re, so it will be enormous at high Reynolds numbers. For the visco-elastic problem the amplification will be of order Wi [60]; hence the effect does exist in the visco-elastic case too, but it is less dramatic in the range 1–10 where the first transitions typically take place.

Transient amplification of initial disturbances is a well-established effect, which in the Newtonian case of the transition to turbulence may well be relate to the Re^{-1} scaling [53] of the threshold amplitude to drive the flow unstable. Nevertheless, the subcritical transition to turbulence is a genuine nonlinear effect, so as long as it has not

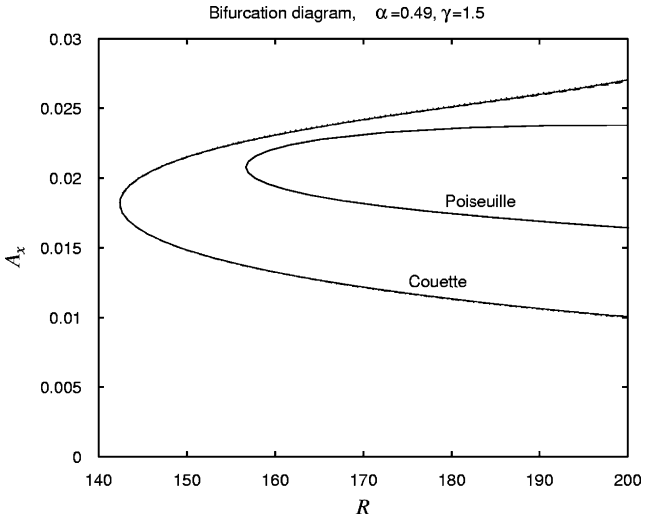

Fig. 18. Phase diagram showing the amplitude A_X of the nonlinear traveling wave solutions of *Newtonian plane Couette and planar Poiseuille* flow in the low-mode approximation of Waleffe [61] as a function of Reynolds number Re. When compared to the exact full nonlinear traveling wave solutions, this approximation is found to be very accurate. Reprinted with permission from Physics of Fluids. Copyright [1997], American Institute of Physics.

been combined with a proper nonlinear analysis it remains a general scenario without, at the moment, much predictive power for the ensuing turbulence.

4.1.4. The self-sustaining cycle scenario for weak turbulence

In the last 10 years, a scenario which is both conceptually important and predictive was developed by Waleffe [62] for the weak Newtonian turbulence in the range where the Reynolds numbers are just large enough that turbulence becomes self-sustained. It has been known since long that in the region just above onset, the weakly turbulent regime has a strong tendency to form so-called *streaks*, thin filamentary regions oriented along the streamwise direction where the streamwise flow is larger or smaller than the average flow at that cross-section.

Moreover, in 1990 Nagata [63] showed, by numerically continuing from the Taylor–Couette flow geometry by increasing the radius of curvature of the cylinders, that there exists a class of *exact nonlinear wavy traveling wave solutions* of plane Couette flow—these solutions are the analogs of the so-called wavy vortex states of Taylor–Couette flow, Taylor vortices which are modulated ("wavy") in the azymuthal direction. Fig. 18 shows the amplitude of these modes as a function of Reynolds number Re in a low-mode approximation [61], for both plane Couette and Poiseuillle flow. Note that these solutions are exact *subcritical* traveling wave solutions which do *not* bifurcate off the laminar base solutions of plane Couette flow or pipe Poiseuille flow through a linear instability, since these flows are linearly stable for all Re.[11]

In the Taylor–Couette geometry, these wavy vortex states are stable in some parameter-range. For plane Couette flow, these states turn out to be linearly unstable, but Waleffe [62] argued that these weakly unstable coherent structures are nevertheless important building blocks of weakly turbulent plane Couette and pipe flow (as well as for wall turbulence). Waleffe argued that the instability of these solutions generates what he termed a *self-sustaining cycle* of three basic types of flow structures: the instability of the nonlinear traveling waves pumps energy into streamwise vortices, a vortex type flow pattern that you see in the normal velocity if you look head on to the flow—see Fig. 19(a). In turn, these streamwise type vortices strongly drive the streaks introduced above, as indicated in Fig. 19(b). And finally a Kelvin–Helmholtz-type instability of the streaks illustrated in Fig. 19(c) drives energy back into the nonlinear traveling coherent wave solutions. This self-sustaining cycle is illustrated in Fig. 20(a). In essence, in this picture self-sustained

[11] These solutions do bifurcate off the laminar flow if an appropriate driving force is added to the Navier–Stokes [61,62]. This is actually used to construct these solutions using continuation methods.

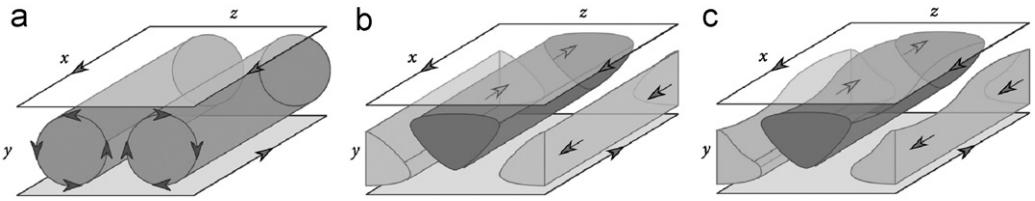

Fig. 19. Illustration of the steps in the self-sustained cycle of Waleffe: streamwise vortices (a) generate streak-like modulations (b). (c) Illustration of the fact that since the streaks generate shear gradients, they experience a finite-wavelength instability similar to the Kelvin–Helmholtz instability of shear layers. Courtesy of J.-W. van de Meent.

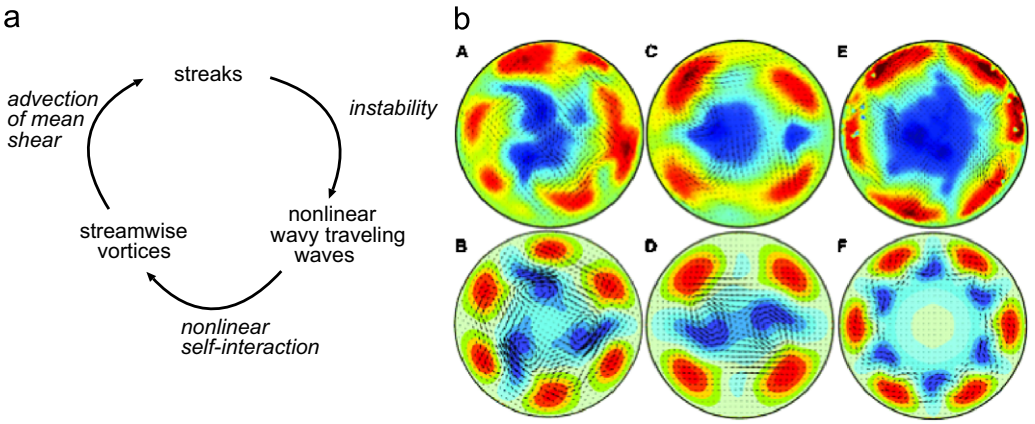

Fig. 20. (a) The "self-sustaining cycle" which according to the theory of Waleffe [62] is responsible for weak turbulence in Newtonian Couette and Poiseuille flows. In a low-mode approximation, the interaction of the various modes reflects the various arrows. (b) Recent experiments and simulations show that weak turbulence in Newtonian pipe flow is exactly due to the interplay of the building blocks identified in (a). Upper row: experimentally measured flow velocities in weakly turbulent pipe flow at $R = 2000$ (A), 2500 (C), 5300 (E); the color coding gives the local speed in the flow direction, with red and blue signifying flow faster or slower than the mean parabolic profile. Thus the colored blobs correspond to the so-called "streaks". The flow in the direction normal to the average flow is indicated by arrows; on close inspection, a vortex-type motion between streaks can be seen. Lower row: corresponding flow states in numerical simulations of the Navier–Stokes equation at $R = 1250$ (B), 1360 (D) and 2900 (F), showing the features found in the experiments and predicted by Waleffe. From Hof et al. [5]. Reprinted with permission from AAAS. Color online.

turbulence occurs when the effective pumping of energy through one cycle exceeds the viscous losses and loss of energy to other modes.

This scenario has been developed in detail by Waleffe [62] by studying the basic features and instabilities of each of these three basic flow structures. Fig. 18 shows the branch of the above-mentioned nonlinear wavy traveling wave states obtained in a Fourier-mode expansion scheme. The mechanism can be worked out explicitly in terms of a simple low-mode expansion which yields a description of weak turbulence in terms of these structures. The coupling of these modes is largely determined by their symmetry and the symmetries of the nonlinear terms in the Navier–Stokes equation, and is summarized by Fig. 20(a). Detailed studies of the various low-mode truncations for weak-turbulence as developed by Waleffe [62] and Moehlis et al. [58] yield explicit predictions for the spectra and various average quantities measured in the weak turbulence.

Very recently, both this qualitative scenario and these quantitative predictions have been confirmed explicitly by experiments [5] and numerical studies [64–66], see Figs. 18 and 19—both in experiments and in simulations, exactly all the ingredients identified by Waleffe's theory are found! It has thus become clear that weak turbulence in parallel shear flows is organized by weakly unstable coherent structures, which regenerate themselves through nonlinear interactions. This in essence dynamical systems scenario, which has some similarities with the mechanism of weakly chaotic behavior in other more simple model systems [52,67], opens up the way to study various other properties, like the stochastic hopping between states with different numbers of streaks, and the boundary of the turbulent attractor [68,64]. That it is a very robust mechanism is also clear from studies of highly compressible flows [69].

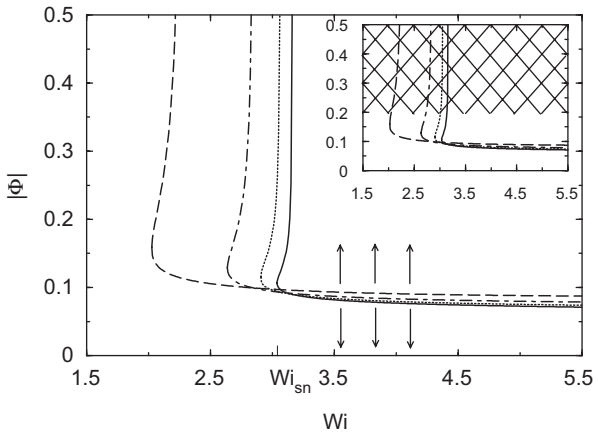

Fig. 21. Subcritical bifurcation diagram for *visco-elastic plane Couette flow* in the UCM (Upper Convected Maxwell) model as determined by our nonlinear amplitude expansion for periodic traveling-wave type solutions. From left to right, the successive lines show the result up to 5th, 7th, 9th and 11th order for $k = 1/d$ and $q = 1/d$ with $2d$ the distance between the plates. Note that the curves appear to converge to a subcritical transition at $\mathrm{Wi}_{\mathrm{sn}} \approx 2.85$.

4.2. Theoretical prediction of a subcritical instability of parallel visco-elastic flows

The arguments presented in Section 3 in favor of the existence of a subcritical nonlinear instability in visco-elastic parallel shear flows have led us to study the nonlinear stability of plane Couette and pipe Poiseuille flow for the Upper Convected Maxwell model (see Section 2.2) using a nonlinear amplitude expansion [18,20]. This amounts to performing an expansion of periodic nonlinear traveling wave states in powers of the amplitude, and probing the stability of these periodic states in successive approximations. Of course, there is no *a priori* guarantee that such an expansion will work, as subcritical bifurcations are notoriously hard to capture perturbatively. Nevertheless, our expectation that the threshold of the nonlinear instability would be sufficiently small at high enough Wi gave us enough hope for success to try such an expansion.

Our results [20] are shown for the Couette flow geometry in Fig. 21. Along the vertical axis, the stationary amplitude A_{shear} of the traveling wave solution is shown. Our normalization is precisely the one introduced in Section 3.5.3: A_{shear} is the maximum value of the periodic modulation of the shear rate at the wall of this mode, divided by the shear rate at the wall of the laminar solution. As is indicated by the arrows, these expansion results completely corroborate our expectation: for the wavenumber shown, periodic modulations are unstable (grow) above some critical values $A^{\mathrm{c}}_{\mathrm{shear}} \simeq 0.11$ when $\mathrm{Wi}_{\mathrm{c}} \gtrsim 2$ in the case of plane Couette flow and when $\mathrm{Wi} \gtrsim 3$ in the case of plane Poiseuille flow [70]. Moreover, as the various dashed curves show, although the results do shift to higher Weissenberg numbers when higher order terms are included in the expansion, the shift of the saddle-node point becomes a factor 2 smaller each time a higher order term is included. The series thus seems to converge. The is especially true for the lower branch, which marks the critical amplitude: These results are very robust as the shift with each successive approximation is small. To our knowledge, the most solid theoretical evidence there is to date for the existence of a subcritical nonlinear instability of the parallel shear flows: a periodic modulation with shear perturbation at the wall of about 11% of that of the base flow is predicted to drive these flows unstable for Wi larger than about 2 in plane Couette flow, about 3 in plane Poiseuille flow, and about 5 in pipe flow.

Note that a critical Wi-value of about 5 for pipe flow is remarkably close to the value where melt fracture type phenomena normally set in, as we discussed in Section 3.6, even though further study is necessary to establish whether this instability is indeed the root cause of most melt fracture type phenomena.

Note that the upper branch of these periodic traveling wave solutions quickly diverges beyond the saddle-node point. We had originally thought that the most likely interpretation of this finding was that our amplitude expansion breaks down at larger amplitudes, as illustrated by the cross-hatched region in the inset of Fig. 21(a). It could also be that this branch of solutions ceases to exist at larger Wi, but it is impossible to assess this within the context of our perturbative

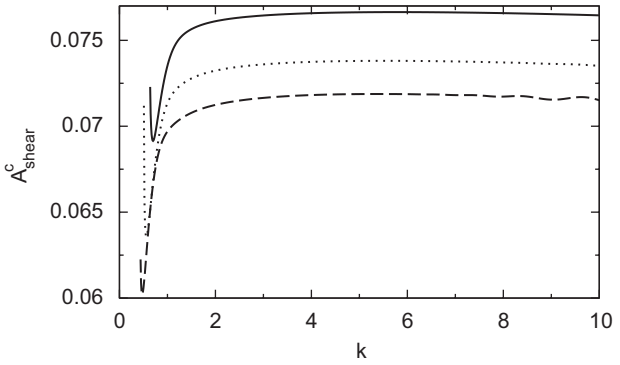

Fig. 22. The critical amplitude A^c_{shear} as a function of the wavenumber k of the periodic perturbation of Couette flow, for $\mathrm{Wi} = 3.0$ (solid line), 3.5 (dotted line), and 4.0 (dashed line).

approach. As we shall see below, the numerical studies of flow do give some indications that the periodic modulations never saturate at a finite amplitude.

We recall that the extension (16) of the Pakdel–McKinley condition discussed in Section 3.5.3 gives a threshold amplitude A^c_{shear} which for fixed wavenumber k should fall off as $1/\mathrm{Wi}^2$. The decay of the threshold amplitude is not very well visible from Fig. 21, but a detailed fit of the threshold amplitude away from the saddle node point is consistent with a power law decay with an exponent somewhat larger than 2 [54]. Fig. 22 shows the critical amplitude A^c_{shear} as a function of k for $\mathrm{Wi} = 3.0, 3.5$, and 4.0 as determined from the amplitude expansion [20]. In agreement with the extension of the Pakdel–McKinley condition, the threshold amplitude is found to be k-independent.

Taken literally, the extended Pakdel–McKinley condition (16) would suggest that there is a finite threshold for every nonzero Wi; this would suggest naievely that the branch of stationary solutions would extend to arbitrarily small Wi, instead of ending in a saddle-node point in Fig. 21. However, as we already indicated in Sections 3.2 and 3.5.3, we consider it most likely that this condition is realistic only for sufficiently large Wi. Indeed, in the Newtonian case it was found that the periodic traveling wave solutions bifurcate from a saddle-node point upon increasing Re, and this suggest that also in the visco-elastic case there is a true saddle-node bifurcation point, as in Fig. 21.

In fact, the branch of periodic traveling wave solutions that we have determined perturbatively in Fig. 21 is indeed essentially the visco-elastic analog of the period traveling wave solutions that Nagata had determined [63] for Newtonian plane Couette flow by continuation methods—compare Fig. 18(a). We have seen that these latter solutions are one of the important building blocks of the self-sustaining cycle scenario for weak Newtonian turbulence. The existence of a similar branch of solutions in the visco-elastic case gives us hope that it may in the near future be possible to develop a similar self-sustaining cycle type scenario for weakly turbulent elastic shear flows.[12] One may well uncover new insight on visco-elastic flows along the way—note in this regard that studies the perturbations of polymers additives to the self-sustaining cycle uncovered the importance of elongational flow in reducing the turbulent drag [71].

We finally note that Doering et al. [60] have recently shown that in plane Couette flow of the UCM model there is no absolute stability for $\mathrm{Wi} > 0.5$ and maybe even less. They considered a special initial condition which consisted of the laminar velocity profile and a constant stress tensor which, however, differed from its laminar values, and showed that for $\mathrm{Wi} > 0.5$ this initial condition exhibits transient growth (see Section 4.1.3). If the perturbation grows strong enough, it could start pumping energy into nontrivial flow modes and lead to turbulence. Although this result is not strong enough to show that parallel visco-elastic shear flows *will* be nonlinearly unstable at some point, it is consistent with the general subcritical nonlinear instability scenario that we advance for sufficiently large Wi.

[12] One note of caution: the fact that we find the transition amplitude to be k-independent away from the saddle-node point, and that the upper branch in Fig. 21 diverges only slightly beyond the saddle-node point, may be an indication that the self-sustained cycle scenario only applies in a rather small range of Weissenberg numbers.

4.3. Numerical evidence for a nonlinear instability

Since for a long time it had not been fully realized that the question of the nonlinear stability of parallel visco-elastic shear flows was a basic open issue, there have not been too many direct studies of such flows. In 2002 Atalik and Keunings [72] have done an extensive study of plane channel flow and plane Couette flow using the Oldroyd-B model and the Giesekus model, with a diffusive term added to the constitutive equation so to enhance numerical stability. In plane Couette flow, they observed stable laminar flow up to $\mathrm{Wi} = 2$; at larger Weissenberg numbers, instabilities developed, but these were attributed to numerical instabilities[13] —compare the remarks at the end of Section 2.2. For plane Poiseuille flow, Atalik and Keunings did observe self-sustained quasi-periodic traveling wave type states, although these persisted to unrealistically small Weissenberg numbers ($\mathrm{Wi} \simeq 0.1$). The precise status of these results therefore does remain unclear.

Recently, Sadanandan and Sureshkumar [73,54] have done a series of precise numerical studies of two-dimensional plane Poiseuille flow in the Oldroyd-B model. These authors did precisely what is necessary to test the subcritical bifurcation scenario: they perturbed the laminar flow with an perturbation proportional to a stable eigenfunction of the linear stability operator, and varied the proportionality factor, the amplitude A of this perturbation. These simulations provide strong support for the subcritical instability scenario that we have advanced: for small A the perturbations decay to zero, in accord with the linear stability of visco-elastic plane Poiseuille flow at small Re. However, beyond some critical value the amplitude of the flow perturbations *grows* rather than decays in time. Fig. 23 illustrates a case at $\mathrm{Wi} = 5$ where the initial disturbance is larger than the critical value. The development in time is in accord with the intuitive idea that once the perturbation is large enough, streamlines are sufficiently perturbed to drive the flow unstable, in accord with the *curvature plus normal stress effects cause instability* picture.

One important finding of these simulations is that when the initial perturbation amplitude is larger than the critical value, the modulation amplitude quickly grows. This is already viable in Fig. 23. It is found, however, that the instability does not saturate: In the numerics, a blow-up in finite time is found. Clearly, there is at present no detailed understanding of this blow-up behavior. Maybe there is indeed no stable finite-amplitude branch of modulated solutions. Note in this regard that our own amplitude expansion results shown in Fig. 21 indeed show the existence of an upper branch of stable modulated solutions only over a small range of Weissenberg numbers just beyond the saddle-node point. However, not too much significance should be attached to this observation, as it could well be that the underlying amplitude expansion simply breaks down at too large amplitudes. If indeed there is no branch of stable traveling wave solutions in two-dimensional plane Poiseuille flow, it may well be that in real three-dimensional simulations, the modulations saturate due to genuine three-dimensional instabilities. For further discussion we refer the reader to [73,54,70].

Recently, Fielding [54,74] has studied the onset of a nonlinear instability in Couette flow using direct numerical simulations with a finite-difference scheme. Her results do confirm, by and large, the existence of a nonlinear instability threshold. However, at the same time they bring up a number of issues which have to be studied in more detail in the future: (i) The nonlinear instability extends to much smaller values (even of order $\mathrm{Wi} \approx 0.5$) than one might expect from the results of our amplitude expansion shown in Fig. 21, on the basis of which we would expect to see no instability below $\mathrm{Wi} \approx 2.85$. This does not necessarily imply a discrepancy, since it is not at all excluded (it is even likely) that there are localized (nonperiodic) perturbations which are different from the periodic ones studied in [20], which can drive the instability.[14] In fact, there are some indications for this, as at least in some cases Fielding finds that there is first a strong transfer of energy from long wavelengths to short wavelength modes, before the eventual instability sets in. Such a mechanism can not be captured by an amplitude expansion which is based on the adiabatic elimination of the short wavelength modes. (ii) In these finite difference simulations, a diffusion type term $L^2\nabla^2\tau_p$ is added to the constitutive equations. The inclusion of such a term is common practice in numerical simulations and is motivated by the idea that the polymer length should provide a short scale cutoff to the constitutive equation. However, both Fielding's numerical studies and the amplitude expansion show that the nonlinear instability threshold when measured in terms of the shear rate modulation at the wall, is strongly increased for values of L larger than about 5×10^{-3}.

[13] It is intriguing to note that according to our expansion results the saddle-node bifurcation point that controls the subcritical instability is at $\mathrm{Wi} \simeq 2.5$—see Fig. 21. Whether the observations of Atalik and Keunings could be a mixed numerical/physical instability has not been investigated.

[14] Moreover, note in this regard that as we have pointed out repeatedly, the extension (16) of the Pakdel–McKinley condition, yields no lower threshold on the nonlinear instability. But as we discussed in Sections 3.2 and 3.5.3, we think it is likely that the condition does not apply for too small Wi. For small Wi, the changes in the normal forces, induced by the flow, have to be taken into account as well.

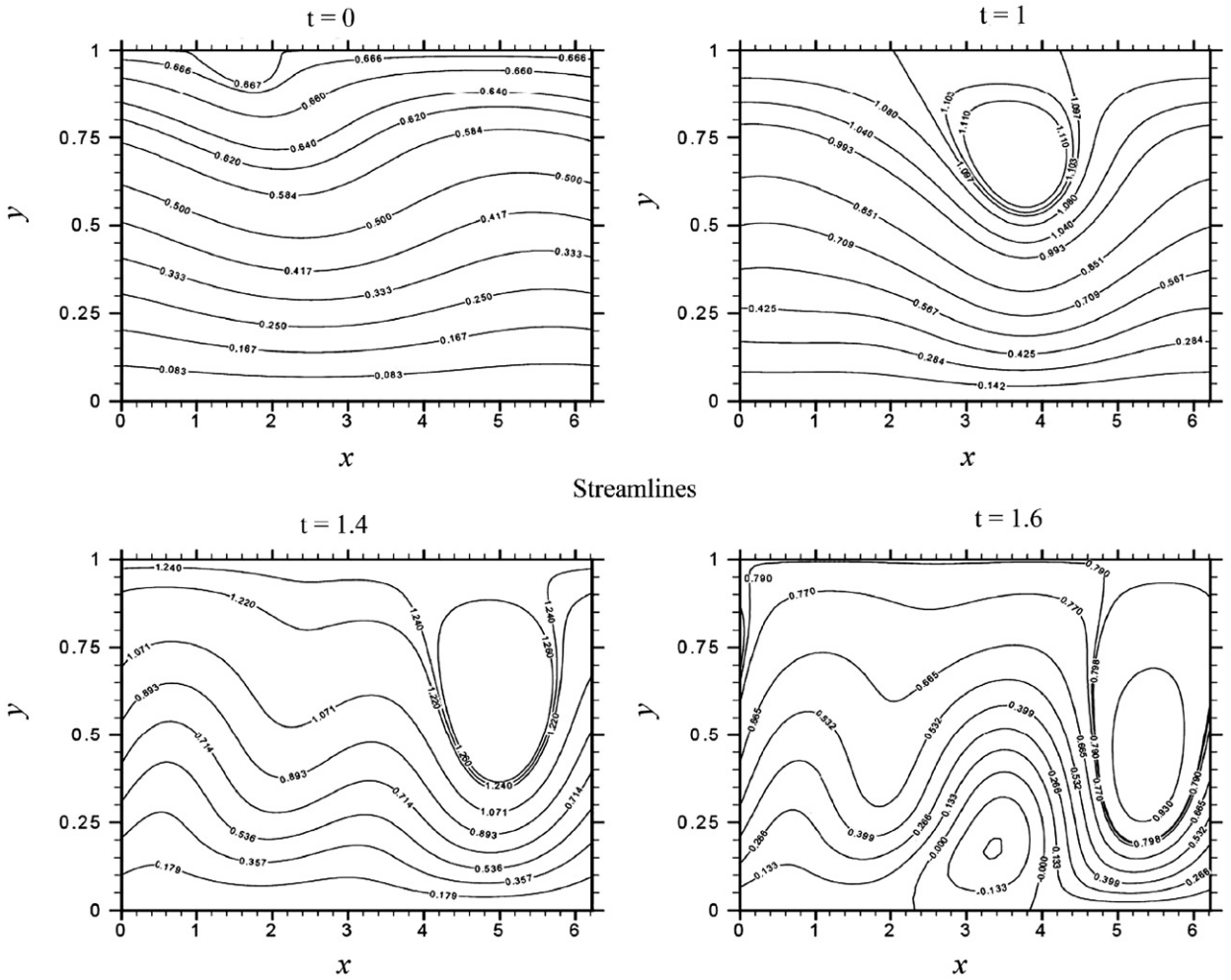

Fig. 23. Simulation of purely elastic two-dimensional plane Poiseuille flow at $\mathrm{Wi} = 5$ by Sadanandan and Sureshkumar [73,54]. The initial finite amplitude perturbation at $t = 0$ grows quickly in size, while it is being advected. Time is measured in units of H/U where H is the distance between the plates and U the mean velocity.

(iii) At small Wi, Fielding finds that the data for all values of L in the range she studied, do fall on a single line when the modulation amplitude is measured in terms of the stress modulation rather than the shear rate modulation. In terms of the stress, the modulation threshold appears to go down as $1/\mathrm{Wi}$. We refer for a further discussion of this to [54].

4.4. The need for controlled experiments: opportunities for micro-rheology

As we mentioned in Section 3.6, there is a lot of circumstantial evidence from observations on melt fracture that low Reynolds number flow in a pipe or through a slit does exhibit a subcritical flow instability. However, in the vast majority of melt fracture experiments the *extrudate* is observed, not the rheology *in* the extruder *before* it flows freely outside. We hope that this article will stimulate new controlled experiments on the nonlinear stability of parallel visco-elastic shear flows.

Experiments near a supercritical bifurcation (see Fig. 14(a)) are normally conceptually straightforward: Since the base flow becomes linearly unstable, and since the branch of nontrivial pattern solutions only exists beyond the bifurcation point, it is difficult to miss the transition—in principle following what happens if one slowly turns up the control parameter is sufficient. Probing a subcritical transition, especially a "bifurcation from infinity" like in Fig. 14(c), is

less trivial, since one needs to apply controlled perturbations to probe it—one may completely miss it if one just waits to see whether anything happens if one turns up the control parameter, since the base state *is* linearly stable. Again the transition to turbulence in Newtonian pipe flows provides a nice illustration of this and of how to proceed in practice. As we mentioned before, in well-controlled experiments one may continue to observe stable laminar flow up to $\mathrm{Re} = \mathcal{O}(10^5)$ or larger, even though if the inlet flow is not carefully controlled turbulence sets in around $\mathrm{Re} = \mathcal{O}(10^3)$. So, in order to study the transition to turbulence and the scaling of the threshold with Re, one has to make sure to design a setup where inlet instabilities are suppressed, and which allows to apply controlled and reproducible perturbations in the bulk [53]. The same will be necessary to explore the nonlinear stability of visco-elastic parallel shear flows.

It is clear that micro-rheology provides exciting new opportunities do these experiments: in micro-rheology the Reynolds number is naturally very small, visualization is simple, and many new techniques have been developed to perturb flows in a controlled way. We therefore hope that the micro-rheology expertise will be brought to bear on this important issue in the near future. Moreover, if the instability is observed in such channel flows, data on the development of the spectra with flow rate would be most welcome.

5. Implications and outlook

The main theme of this paper is that while visco-elastic fluids may exhibit nontrivial but coherent patterns in a small range of Weissenberg numbers, the rheology of these fluids has a strong tendency to rapidly become turbulent. If we compare this in the spirit of Fig. 1 with the behavior of Newtonian fluids as a function of Reynolds number, the most striking differences appear to be that the range of coherent flows appears to be smaller in visco-elastic fluids than in regular fluids, and that visco-elastic fluids show an even stronger tendency to subcritical behavior. We conclude from this that the possibility of polymers to load energy through stretching in regions of high shear, and to give off this energy in regions of lesser shear, tends to be a self-enhancing effect that drives incoherent flow.

Till recently the most solid evidence for this picture came from a series of well-controlled experiments performed over the last couple of years. But, as we have discussed, very recent theoretical and numerical investigations do support the proposed scenario that parallel shear flows also exhibit a nonlinear subcritical instability, even though a number of details still remain to be sorted out. Moreover, the idea of a subcritical instability in these flows is completely in line with the accepted idea that curved streamlines together with normal stress effects tend to give *linear instabilities*. Even if there is a true linear instability in laminar flows due to the curvature of the streamlines, the instability tends to be subcritical, i.e., to be enhanced by the nonlinear pumping. If the streamlines of the base flow are straight, there is no linear instability, but the nonlinear pumping will typically still cause a *nonlinear instability*: Once the flow is perturbed by a sufficiently large finite amount, the perturbed streamlines are curved, and hence unstable. The extension of the original linear instability criterion of Pakdel and McKinley to these subcritical nonlinear instabilities, implements this idea. The extended criterion is fully supported by the amplitude expansion calculations, and strongly suggests that high Weissenberg number flows show a strong tendency to become turbulence [54], since the threshold is predicted to rapidly go down as $1/\mathrm{Wi}^2$.

The above conclusion has many implications. The good news is that studies of visco-elastic turbulence becomes all the more relevant, and theories of visco-elastic turbulence ([48] and references therein) may have quite a large range of applicability. The bad news, unfortunately is, that while the equations describing the rheology of visco-elastic fluids are already quite difficult to handle, the implication from the above is that linear stability analysis and weakly nonlinear methods like amplitude expansions, are likely to be of very limited use.

From a more general perspective, this conclusion may also have important implications for our understanding of *shear banding*, the fact that sheared complex fluids may tend to break up into zones with very different shear rates [75,76]. Almost all of our theoretical understanding of shear banding is based on the *assumption* that the flow within each of these zones remains laminar. If, however, nonlinear flow instabilities occur in these zones, we expect these to couple strongly to the shear banding itself [77,78]. There are already experimental indications for this [79].

A second important indirect implication of our general conclusion is for numerical simulations. As we discussed briefly in Section 2.2, simulations of visco-elastic flows are prone to numerical instabilities, the so-called High Weissenberg Number Problem. These problems already tend to show up in simulations of coherent but laminar flow profiles. However, if the fluid itself can also show sudden strong instabilities to nontrivial flows with strongly sheared regions, it will not be easy to disentangle these from true physical instabilities. Maybe in some cases a true physical instability

drives what appears to be a numerical instability. But even when there are true numerical instabilities, the occurrence of additional physical instabilities will certainly exacerbate the problem.

Finally, as we mentioned, the field of micro-fluidics seems to bring new opportunities to test some of these nonlinear instabilities. At the same time, the strong tendency of visco-elastic fluids to become turbulent at small Reynolds numbers may help solve the mixing problem in micro-fluidics.

Acknowledgements

We are grateful to a large number of colleagues for illuminating discussions, remarks and collaborations over a number of years since we started working on this line of research: Paul Becherer, Daniel Bonn, Morton Denn, Bruno Eckhardt, Suzanne Fielding, Alexander Groisman, Timon Idema, Roland Keunings, Rick Kerswell, Ron Larson, Bernard Meulenbroek, Peter Olmsted, Anshuman Roy, Victor Steinberg, Kees Storm, Eric Sultan, Radhakrishna Sureshkumar, Patrick Tabeling, Jan Willem van de Meent, Christian Wagner, and Dave Weitz.

References

[1] R.C. DiPrima, H.L. Swinney, Instabilities and transition in flow between concentric rotating cylinders, in: H.L. Swinney, J.P. Gollub (Eds.), Hydrodynamic Instabilities and the Transition to Turbulence, Springer, New York, 1981.
[2] H.L. Swinney, Instabilities and chaos in rotating fluids, in: G. Gallavotti, P.F. Zweifel (Eds.), Nonlinear Evolution and Chaotic Phenomena. Proceedings of a NATO Advanced Study Institute, Plenum, New York, 1988, pp. 319–326.
[3] C.D. Andereck, S.S. Liu, H.L. Swinney, Flow regimes in a circular Couette system with independently rotating cylinders, J. Fluid Mech. 164 (1986) 155–183.
[4] P.J. Schmid, D.S. Henningson, Stability and Transition in Shear Flows, Springer, New York, 2001.
[5] B. Hof, C.W.H. van Doorne, J. Westerweel, F.T.M. Nieuwstadt, H. Faisst, B. Eckhardt, H. Wedin, R.R. Kerswell, F. Waleffe, Experimental observation of nonlinear traveling waves in turbulent pipe flow, Science 305 (2004) 1594.
[6] R.B. Bird, R.C. Armstrong, O. Hassager, Dynamics of Polymeric Liquids, Wiley, New York, 1987.
[7] M.M. Denn, Issues in visco-elastic fluid mechanics, Annu. Rev. Fluid Mech. 13 (1990) 13.
[8] M.M. Denn, Fifty years of non-Newtonian fluid dynamics, A.I.Ch.E.J. 50 (2004) 2335–2345.
[9] E.S.G. Shaqfeh, Purely elastic instabilities in viscometric flows, Ann. Rev. Fluid Mech. 28 (1996) 129.
[10] R.G. Larson, The Structure and Rheology of Complex Fluids, Oxford University Press, Oxford, 1999.
[11] R.G. Larson, Constitutive Equations for Polymer Melts and Solutions, AT&T Bell Laboratories, 1988.
[12] R.G. Owens, T.N. Phillips, Computational Rheology, Imperial College Press, London, 2002.
[13] R. Fattal, R. Kupferman, Constitutive laws for the matrix-logarithm of the conformation tensor, J. Non-Newtonian Fluid Mech. 123 (2004) 281–285.
[14] M.A. Hulsen, R. Fattal, R. Kupferman, Flow of viscoelastic fluids past a cylinder at high Weissenberg number: stabilized simulations using matrix logarithms, J. Non-Newtonian Fluid Mech. 127 (2005) 27–39.
[15] P. Pakdel, G.H. McKinley, Elastic instability and curved streamlines, Phys. Rev. Lett. 77 (1996) 2459.
[16] G.H. McKinley, P. Pakdel, A. Öztekin, Rheological and geometric scaling of purely elastic flow instabilities, J. Non-Newtonian Fluid Mech. 67 (1996) 19–47.
[17] V. Bertola, B. Meulenbroek, C. Wagner, C. Storm, A. Morozov, W. van Saarloos, D. Bonn, Melt fracture in polymer extrusion, Phys. Rev. Lett. 90 (2003) 114502.
[18] B. Meulenbroek, C. Storm, V. Bertola, C. Wagner, D. Bonn, W. van Saarloos, Intrinsic route to melt fracture in polymer extrusion: a weakly nonlinear subcritical instability of visco-elastic Poiseuille flow, Phys. Rev. Lett. 90 (2003) 024502.
[19] B. Meulenbroek, C. Storm, A.N. Morozov, W. van Saarloos, Weakly nonlinear subcritical instability of visco-elastic Poiseuille flow, J. Non-Newtonian Fluid Mech. 116 (2004) 235.
[20] A.N. Morozov, W. van Saarloos, Subcritical finite-amplitude solutions in plane Couette flow of visco-elastic fluids, Phys. Rev. Lett. 95 (2005) 024501.
[21] G.V. Vinogradov, V.N. Manin, An experimental study of elastic turbulence, Kolloid Z. 201 (1965) 93.
[22] A. Groisman, V. Steinberg, Elastic turbulence in a polymer solution flow, Nature 405 (2000) 53.
[23] A. Groisman, V. Steinberg, Efficient mixing at low Reynolds numbers using polymer additives, Nature 410 (2001) 905.
[24] A. Groisman, V. Steinberg, Elastic turbulence in curvilinear flows of polymer solutions, N. J. Phys. 6 (art. no. 29) (2004).
[25] T. Burghelea, E. Segre, V. Steinberg, Elastic turbulence in von Karman swirling flow between two disks, Phys. Fluids, submitted for publication, physics/0609112.
[26] R.G. Larson, Turbulence without intertia, Nature 405 (2000) 27.
[27] M. Pahl, W. Gleissle, H.-M. Laun, Praktische Rheologie der Kunststoffe und Elastomere, VDI verlag, 1991.
[28] M.M. Denn, Extrusion instabilities and wall slip, Annu. Rev. Fluid Mech. 33 (2001) 265.
[29] R.J. Koopmans, J. Molenaar, Polymer Melt Fracture: the Search for Solutions to Polymer Melt Flow Instabilities, Marcel Dekker, New York, to appear.
[30] C. Rauwendaal, P.J. Gramann, Polymer Extrusion, Hanser, Munich, 2001.

[31] J.L. Lumley, Drag reduction by additives, Ann. Rev. Fluid Mech. 1 (1969) 367.
[32] P.S. Virk, Drag reduction fundamentals, A.I.Ch.E.J. 21 (1975) 625.
[33] A. Gyr, H.W. Bewersdoff, Drag Reduction of Turbulent Flows by Additives, Kluwer, Dordrecht, 1995.
[34] P.G. de Gennes, Introduction to Polymer Dynamics, Cambridge University Press, Cambridge, 1990.
[35] M. Doi, S.F. Edwards, The Theory of Polymer Dynamics, Clarendon Press, Oxford, 1986.
[36] D.V. Boger, Highly elastic constant-viscosity fluid, J. Non-Newtonian Fluid Mech. 3 (1977) 87.
[37] R.I. Tanner, K. Walters, Rheology: A Historical Perspective, Elsevier, Amsterdam, 1998.
[38] R.G. Larson, E.S.G. Shaqfeh, S.J. Muller, A purely elastic instability in Taylor–Couette flow, J. Fluid Mech. 218 (1990) 573.
[39] V.A. Gorodtsov, A.I. Leonov, On a linear instability of a plane parallel Couette flow of viscoelastic fluid, J. Appl. Math. Mech. 31 (1967) 310.
[40] T.C. Ho, M.M. Denn, Stability of plane poiseuille flow of a highly elastic liquid, J. Non-Newtonian Fluid Mech. 3 (1978) 179.
[41] Y.L. Joo, E.S.G. Shaqfeh, A purely elastic instability in Dean and Taylor-Dean flow, Phys. Fluids A 4 (1992) 524–543.
[42] A. Groisman, V. Steinberg, Mechanism of elastic instability in Couette flow of polymer solutions: experiments, Phys. Fluids 10 (1998) 2451.
[43] A. Öztekin, B. Alakus, G.H. McKinley, Stability of planar stagnation flow of a highly viscoelastic fluid, J. Non-Newtonian Fluid Mech. 72 (1997) 1–29.
[44] J.A. Byars, A. Öztekin, R.A. Brown, G.H. McKinley, Spiral instabilities in the flow of highly elastic fluids between rotating parallel disks, J. Fluid Mech. 271 (1994) 173–218.
[45] A. Morozov, T. Idema, W. van Saarloos, in press.
[46] A. Öztekin, R.A. Brown, Instability of a visco-elastic fluid between rotating parallel disks: analysis for the Oldroyd-B fluid, J. Fluid Mech. 255 (1993) 473.
[47] B.A. Schiamberg, L.T. Shereda, H. Hu, R.G. Larson, Transitional pathway to elastic turbulence in torsional, parallel-plate flow of a polymer solution, J. Fluid Mech. 554 (2006) 191–216.
[48] A. Fouxon, V. Lebedev, Spectra of turbulence in dilute polymer solutions, Phys. Fluids 15 (2003) 2060–2072.
[49] M.C. Cross, P.C. Hohenberg, Pattern formation outside of equilibrium, Rev. Mod. Phys. 65 (1993) 851.
[50] L.M. Pismen, Patterns and Interfaces in Dissipative Dynamics, Springer, Berlin, 2006.
[51] C. Godrèche, P. Manneville (Eds.), Hydrodynamics and Nonlinear Instabilities, Cambridge University Press, Cambridge, 1998.
[52] M. van Hecke, M. Howard, Ordered and self-disordered dynamics of holes and defects in the one-dimensional complex Ginzburg–Landau equation, Phys. Rev. Lett. 86 (2001) 2018–2021.
[53] B. Hof, A. Juel, T. Mullin, Scaling of the turbulence transition threshold in a pipe, Phys. Rev. Lett. 91 (2003) 244502 and references therein.
[54] A.N. Morozov, S. Fielding, B. Sadanandan, R. Sureshkumar, W. van Saarloos, Polymer parallel shear flows are prone to nonlinear elastic instabilities that drive them turbulent, Nature, submitted for publication.
[55] L. Robert, Instabilite oscillante de polyethylenes linearises: observations et interpretations, Ph.D. Thesis, University of Nice, 2001.
[56] F. Waleffe, Transition in shear flows—nonlinear normality versus nonnormal linearity, Phys. Fluids 7 (1995) 3060–3066.
[57] S.J. Chapman, Subcritical transition in channel flows, J. Fluid Mech. 451 (2002) 35–97.
[58] J. Moehlis, H. Faisst, B. Eckhardt, A low-dimensional model for turbulent shear flows, N. J. Phys. 6 (2004) 56.
[59] L.N. Trefethen, A.E. Trefethen, S.C. Reddy, T.A. Driscoll, Hydrodynamic stability without eigenvalues, Science 261 (1993) 578–584.
[60] C.R. Doering, B. Eckhardt, J. Schumacher, Failure of energy stability in Oldroyd-B fluids at arbitrarily low Reynolds numbers, J. Non-Newtonian Fluid Mech. 135 (2006) 92.
[61] F. Waleffe, Three-dimensional coherent states in plane shear flows, Phys. Rev. Lett. 81 (1998) 4140.
[62] F. Waleffe, On a self-sustaining process in shear flows, Phys. Fluids 9 (1997) 883–900.
[63] M. Nagata, Three-dimensional finite-amplitude solutions in plane Couette flow: bifurcation from infinity, J. Fluid Mech. 217 (1990) 519.
[64] H. Faisst, B. Eckhardt, Travelling waves in pipe flows, Phys. Rev. Lett. 90 (2003) 224502.
[65] H. Wedin, R.R. Kerswell, Exact coherent structures in pipe flow: travelling wave solutions, J. Fluid Mech. 508 (2004) 333–371.
[66] R.R. Kerswell, Recent progress in understanding the transition to turbulence in a pipe, Nonlinearity 18 (2005) R17–R44.
[67] K. Kaneko, I. Tsuda, Chaotic itinerancy, Chaos 13 (2003) 926–936.
[68] J. Moehlis, H. Faisst, B. Eckhardt, Periodic orbits and chaotic sets in a low-dimensional model for shear flows, SIAM J. Appl. Dyn. Systems 4 (2005) 352–376.
[69] J.W. van de Meent, A. Morozov, E. Sultan, E. Somfai, W. van Saarloos, in preparation.
[70] A.N. Morozov, W. van Saarloos, in preparation.
[71] A. Roy, A. N. Morozov, W. van Saarloos, R. Larson, Mechanism of polymer drag reduction using a low-dimensional model, Phys. Rev. Lett. 97 (2006) 234501.
[72] K. Atalik, R. Keunings, Non-linear temporal stability analysis of visco-elastic plane channel flows using a fully-spectral method, J. Non-Newtonian Fluid Mech. 102 (2002) 299.
[73] B. Sadanandan, Ph.D. Thesis, University of Washington in St. Louis, 2004.
[74] S. Fielding, unpublished.
[75] O. Diat, D. Roux, F. Nallet, Effect of shear on a lyotropic lamellar phase, J. Phys. II (France) 3 (1993) 1427–1452.
[76] J.-F. Berret, Rheology of Wormlike Micelles: Equilibrium Properties and Shear Banding Transition, cond-mat/0406681.
[77] S.M. Fielding, Linear instability of planar shear banded flow, Phys. Rev. Lett. 95 (2005) 134501.
[78] S.M. Fielding, P.D. Olmsted, Nonlinear dynamics of an interface between shear bands, Phys. Rev. Lett. 96 (2006) 104502.
[79] S. Lerouge, M. Argentina, J.P. Decruppe, Interface instability in shear-banding flow, Phys. Rev. Lett. 96 (2006) 088301.